processes

MDPI

Article

Processing of Ilmenite Concentrate with High Chromium Content

Bagdaulet Kenzhaliyev, Almagul Ultarakova *, Azamat Toishybek and Nurzhan Sadykov

The Institute of Metallurgy and Ore Beneficiation, Satbayev University, Almaty 050013, Kazakhstan
* Correspondence: a.ultarakova@satbayev.university; Tel.: +7-707-3218321

Abstract: The results of research on the processing of ilmenite concentrate from the Obukhovskoye deposit are presented in this article. As the concentrate has a high chromium content, the study involved converting the iron into metal and the titanium into slag through the addition of soda. Positive results were obtained during the smelting of the ilmenite concentrate, and a one-stage smelting mode was established. This mode involved an increase in the temperature up to 1700 °C, with a heating step of 10 °C/min and using an argon supply. The holding time at this temperature was 30 min, followed by cooling to 700 °C in argon. The optimal parameters for sintering the non-magnetic fraction with soda and leaching the sinter with water and hydrochloric acid solution were also determined.

Keywords: ilmenite; reduction smelting; magnetic fraction; non-magnetic fraction; chromium; titanium

1. Introduction

Global practices of titanium sponge production mainly use two minerals: ilmenite $FeTiO_3$ and rutile TiO_2. Ilmenite is the most widespread titanium mineral and is a source of synthetic rutile, which is used in the production of pigments and metallic titanium [1]. The Republic of Kazakhstan ranks No. 3 in the world in terms of the production of products required in the aerospace sector. The Ust-Kamenogorsk Titanium and Magnesium Plant (UKTMP JSC) is one of the world's largest vertically integrated producers of TG-100 titanium sponge.

The UKTMP JSC facility has modern technological equipment and produces high-grade titanium sponges that are used to produce titanium ingots, alloys, and rolled products. The consumers of these products are aerospace companies, such as Boeing, Airbus, Rolls-Royce, Pratt and Whitney, and General Electric. The expansion of titanium slag production and the range of titanium ingots, alloys, rolled products, titanium-coated products, and other titanium products from UKTMP JSC depends on its titanium sponge output and, above all, its output of high-quality ilmenite concentrates [2,3].

Deposits of placers and weathering crusts, which formed as a result of the denudation of bedrock in coastal marine and continental conditions of sedimentation, form the mineral resource base of titanium–zirconium ores in the Republic of Kazakhstan. Titanium–zirconium placers and weathering crusts usually have low average contents of the main useful components (rutile, ilmenite, and zircon), and contain the associated mineralization of valuable rare and rare-earth elements [4–6].

The recovery of pure ilmenite concentrates from deposits is often challenging, due to the existence of chromium-containing impurities. Even the existence of a small amount of chromium in ilmenite concentrates reduces their market value as a potential raw material for the production of pigments based on titanium dioxide. For these reasons, there is a need for the preliminary deep purification of these concentrates from chromium [7]. The main forms of chromium impurities in ilmenite concentrates are Cr_2O_3 (chromium-containing) spinel minerals (i.e., chromium-rich spinels), such as chromite $FeCr_2O_4$, magnesiochromite $MgCr_2O_4$, and aluminochromite $(Fe,Mg)(Cr,Al)_2O_4$. In current industrial

check for updates

Citation: Kenzhaliyev, B.; Ultarakova, A.; Toishybek, A.; Sadykov, N. Processing of Ilmenite Concentrate with High Chromium Content. *Processes* **2024**, *12*, 1462. https://doi.org/10.3390/pr12071462

Academic Editor: Carlos Sierra Fernández

Received: 16 April 2024
Revised: 5 July 2024
Accepted: 11 July 2024
Published: 12 July 2024

practices, chromium impurities are separated from ilmenite concentrates through a magnetization roasting process [8,9]. At present, there is a trend toward the processing of low-grade titanium deposits, due to a decline in the quality of primary ores around the world.

The high chromium content in ilmenite concentrates makes it difficult to further process them into titanium-containing slag, titanium tetrachloride, and sponge titanium, as its presence causes problems with chromium transfer into the final products. In this regard, there is a need to purify both the concentrates and products of ilmenite processing to remove the chromium [10,11].

Currently, about 4.5 thousand tons of waste ilmenite concentrate has accumulated at the beneficiation plant of Tioline LLP, which processes the titanium–zircon placers of the Obukhovskoye deposit, due to the plant's non-compliance with technical requirements because of the deposit's high content of chromium, making titanium alloys and ingots cold-short [12]. The ilmenite concentrate of the Obukhovskoye deposit contains 54.89–56.0% TiO_2, 27.35–30.2% Fe_2O_3, and 2.7–6.4% Cr_2O_3, whereas the chromium oxide content should not exceed 2% Cr_2O_3 in the case of the ilmenite concentrates that are supplied for processing by UKTMP JSC. In turn, the chromium content in titanium slags should not exceed 0.1% Cr_2O_3 [13].

In existing industrial practice, chromium impurities are separated from ilmenite concentrates using a magnetization roasting process [14–17]. In global practice, the development of the roasting–magnetic separation of ilmenite concentrates began with the use of oxidative roasting for unaltered ilmenites from primary deposits and gas-reducing roasting for highly altered ilmenites from placer deposits. As most deposits contain ilmenite grains of various alteration degrees, this study aimed to develop an effective universal method of carbon-thermal reduction in tubular rotary furnaces, with subsequent cooling in a controlled atmosphere. Catalytic additives comprising the salts of alkaline earth metals and other elements and compounds are used to reduce the temperature and increase the reduction degree and coagulation of iron [18–22]. Metallic iron is extracted from sinters using magnetic separation and from non-magnetic fractions by leaching. The purity of artificial rutile directly depends on the purity of the initial ilmenite concentrate and the degree of iron metallization. The calcination of ilmenite concentrates under oxidizing or reducing conditions increases the magnetic susceptibility of ilmenite, which, in combination with magnetic separation, favors its separation into a monomineral fraction [23,24].

In [25–28], the authors investigated an ilmenite concentrate with a high chromium content from the Murray Basin deposit. As a result, the authors found that slightly diluted ilmenite concentrates contained fine-grained associations of ilmenite and pseudorutile. Ilmenite with a content of 0.1 wt.% Cr_2O_3 was subjected to magnetization roasting at low temperatures (650 °C) in an environment of slightly fluidized gases. A gas mixture of N_2, CO_2, and H_2O, simulating completely burned natural gas, was effective as a fluidizing gas. It was found that the addition of small amounts (1–2 vol.%) of hydrogen or oxygen to the fully burned gas mixture had a negative effect on the removal of chromium from altered ilmenite concentrates during weathering, increasing the residual Cr_2O_3 content to 0.1 wt.% in the magnetic product.

An alternative method for the disposal of these low-grade ilmenite concentrates is to process them into TiO_2 slag by direct smelting, as their high iron content provides suitable thermodynamic conditions for smelting. However, the direct smelting of ilmenite fines is quite challenging due to environmental issues and improper smelting, which results in higher production costs. Therefore, it is necessary to grind these low-grade ilmenite fines into ilmenite granules before the smelting process to use them economically [29–32].

Thus, the purpose of this study, which is focused on the processing of leucoxenized ilmenite concentrates with increased contents of chromium, is to develop a method of pyrometallurgical treatment for the maximum conversion of iron and chromium into the metal fraction and titanium into the slag fraction, with the further removal of chromium from the titanium-containing fraction.

2. Materials and Methods

Materials and equipment: The chemical composition of the substandard ilmenite concentrate sample from the Obukhovskoye deposit in the Republic of Kazakhstan is presented in Table 1. The ilmenite concentrate has a density of 4.29 g/cm^3 and a bulk mass of 1.95 g/cm^3; its particle size distribution is also presented in Table 2. An analytical grade of Na_2CO_3 was used for roasting and smelting.

Table 1. Chemical composition of ilmenite concentrate (wt.%).

Name	TiO_2	FeO	Fe_2O_3	Cr_2O_5	Al_2O_3	SiO_2	MgO	MnO_2	P_2O_5	SO_3	ΣREE
Ilmenite concentrate	61.6	3.0	25.6	4.1	1.1	0.86	1.5	1.5	0.07	0.03	0.64

Table 2. Particle size distribution of ilmenite concentrate.

Classes, mm	Exit, %
+0.1	0.14
−0.1 + 0.071	61.9
−0.071 + 0.05	37.05
−0.05 + 0.045	0.62
−0.045 + 0.0	0.3
Total:	100.0

According to the particle size distribution, ilmenite from the Obukhovskoye deposit is of the fine-grained type. According to the results of the sieve analysis, it was found that 98.95% of the ilmenite concentrate is fine-grained material, with a grain size of −0.1 + 0.05 mm. A sludge yield of −0.05 + 0 mm accounts for 0.92% of the concentrate.

Coke from Sary-Arka JSC was used to carry out the pyrometallurgical analysis, the qualitative characteristics of which are presented in Table 3. The composition of the coke ash is shown in Table 4.

Table 3. Qualitative characteristics of coal coke from the Sary-Arka JSC.

Indicators	Designation	wt.%
Ash content on a dry basis	A	4.3
Volatile matter	V	3.7
Moisture	W	3.0
Sulfur total	S	0.1
Fixed carbon	C	86.2
Phosphorus	P	0.01
Net calorific value	Q	31,400 kJ/kg
Particle size	-	5–25 mm

Table 4. Composition of coke ash from Sary-Arka JSC.

	Fe_2O_3	CaO	SiO_2	Al_2O_3	MgO	K_2O	Na_2O	SO_3	P_2O_5
Ash, wt.%	9.2	2.5	54.3	25.8	1.6	2.5	1.2	2.4	0.5

Coke obtained from coal from the Shubarkolskoye deposit is considered active and low in ash. It has a well-developed pore structure formed of both large pores (150–300 microns in size) and small pores (0 to 1.0 microns in size). The coke was crushed on a vibrating abrasive IV1 (VIBROTECHNIK LLC, St. Petersburg, Russia) to 0.074 mm.

Oxidizing and reducing roasting were performed. A charge was prepared without the addition of soda ash, with a composition of 82% ilmenite concentrate, 17% coke, and 1% molasses. The ilmenite concentrate of the Obukhovskoye deposit was ground up to a size class of 0.074 mm on a vibrating abrasive IV 1. Large pieces of coke were crushed to fractions of −0.5 + 0.1 mm and were then thoroughly mixed with the crushed ilmenite concentrate and binder. Then, the prepared mass was transferred into cylindrical steel molds, and briquettes with a size of 16 × 19 mm were formed. The briquettes were dried in a muffle furnace at 60–70 °C for 180 min. A charge was prepared from the ilmenite concentrate and coke, with the addition of soda ash from the initial concentrate. Molasses was used as the binder for the briquettes. Their chemical composition is shown in Table 5. Molasses is a syrupy liquid with a dark brown color. Molasses is often used in laboratory studies as a binder for the manufacture of briquettes from charge materials. The addition of soda contributes to the liquefaction of slag, as a result of the formation of medium-smelting aluminosilicates and sodium titanates [12]. With the addition of 4% soda, the charge had the following composition: 78% ilmenite concentrate, 17% special coke, 4% soda, and 1% molasses. During the preparation of the charge, the ilmenite concentrate was also ground down.

Table 5. Chemical composition of the binder (wt.%).

The Binder	C	H	O	SiO_2	K_2O	Na_2O	MgO	CaO	N	SO_3	P_2O_5
Molasses	38.71	6.0	48.0	0.5	2.6	0.02	1.2	1.6	1.3	0.03	0.04

Three briquettes were placed in a graphite crucible, and coke was placed at the bottom of the crucible. The briquettes were roasted in a chamber furnace (Kejia, Zhengzhou, China). Oxidative roasting was performed in three stages at 900 °C, 1000 °C, and 1100 °C, and roasting was performed without and with the addition of 4% and 6% calcined soda at each temperature. The charge with the addition of 6% soda had the following composition: 76% ilmenite concentrate, 17% coke, 6% soda, and 1% molasses. The sinter was pulverized after roasting, and magnetic separation was performed with an AMR brand magnet (Scientific and Production Company "Prodekologia" No. 0888, dated 07.2017, Ukraine) at a magnetic field strength of 200 Oersted. The extraction was calculated using the following formula:

$$\varepsilon = \beta \times Q/\gamma \times P \times 100\%, \quad (1)$$

where ε—extraction of the calculated component in the product, %; where β—content of the component in the obtained product, wt.%, Q—yield (mass) of the obtained product, g, γ—content of the component in the initial product, wt.%, P—mass of the initial product, g.

Reduction roasting with and without the addition of 4% and 6% calcined soda in the ilmenite concentrate was conducted at 1000 °C. The preparation of the charge and briquettes was similar to that for the oxidative roasting. The furnace regime of the reducing roasting was similar to that of the oxidative roasting but was performed in a reducing atmosphere with the presence of argon.

Reduction smelting at 1600 °C and 1700 °C was also performed. Two-stage smelting at 1600 °C was conducted in a tubular, vertical, high-temperature RHTV 120,600/C Nabertherm furnace (Nabertherm GmbH, Lilienthal, Germany). The charge consisted of 77% ilmenite concentrate, 6% soda ash, and 17% coke. Reduction smelting at 1700 °C (Figure 1) was performed in an XY-1800 chamber furnace (Henan Super Machinery Equipment Co., Ltd., Zhengzhou, China). The charge consisted of 66% ilmenite concentrate, 20% magnetic fraction, 6% soda ash, 7% coke, and 1% molasses.

Figure 1. Preparation of briquettes for smelting at 1700 °C.

Preparation of the slag fraction consisted of grinding the material on an IV6 vibrating abrasion machine up to 0.044 mm. The slag fraction was sintered with soda in the Kejia chamber furnace. The sinter was leached with hot water that was heated using a laboratory magnetic stirrer AREC (VELP Scientifica Srl., Usmate Velate, Italy) in the mixing device VELP LS (VELP Scientifica Srl., Italy). Filtration was carried out using a Buchner funnel and a Bunsen flask, and the vacuum was created with the BC-VP-4P vacuum pump (Value, Wenling, China).

Analysis methods. The quantitative contents of the main elements in the solutions and solid samples were determined using an Optima 8300DV atomic emission spectrometer with inductively coupled plasma (PerkinElmer, Inc., Waltham, MA, USA) and an AA-7000 atomic absorption spectrometer (Shimadzu, Kyoto, Japan). X-ray phase analysis was performed on a D8 ADVANCE diffractometer (BRUKER AXS GmbH, Karlsruhe, Germany) with Cu–Kα radiation, using the PDF-2 database of the International Center for Diffraction Data ICDD (USA). X-ray fluorescence analysis was performed on a Venus 200 PANalytical B.V spectrometer with wave dispersion (Malvern Panalytical, Almelo, The Netherlands). The polished briquettes were studied using a LEICADM 2500 P (Leica Microsystems GmbH, Wetzlar, Germany) microscope. The ilmenite was also studied with an OLYMPUS BX51 (Olympus, Tokyo, Japan) optical microscope. The compositions of the mineral phases were determined using the JEOL JXA 8230 electron probe microanalyzer (JEOL Ltd., Tokyo, Japan)

3. Results and Discussion

3.1. Oxidative Roasting Process for Ilmenite Concentrate

The phase analysis of the original concentrate is shown in Figure 2. The main phases of the ilmenite concentrate include ilmenite, rutile, and pseudorutile.

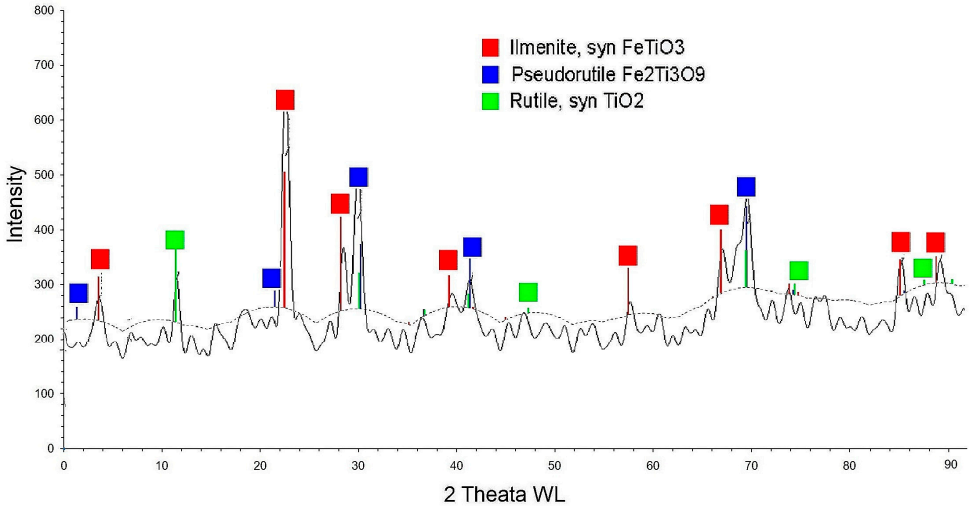

Figure 2. X-ray diffraction pattern of ilmenite concentrate.

The results of the SEM-EDS elemental mapping of ilmenite concentrate are shown in Figure 3. As shown in Figure 3, ilmenite ($FeO{\cdot}TiO_2$) is a grey mineral of high hardness with clear reflectivity and strong anisotropy. Titanium in its oxide form is present in the tetravalent form in practically all natural minerals and is most often associated with iron oxides of different valences. The most common titanium minerals are ilmenite ($FeTiO_3$) and leucoxene ($TiO_2{\cdot}nH_2O{\cdot}Fe_2O_3$), including hematite, which is formed as a result of weathering or from the oxidation of ilmenite or other titanium minerals. The ilmenite lattice changes and is rearranged, after which pseudobrookite ($Fe_2O_3{\cdot}TiO_2$), then arizonite ($Fe_2O_3{\cdot}3TiO_2$), and the aforementioned altered leucoxene appear in the next stages in hydrothermal and oxidizing environments.

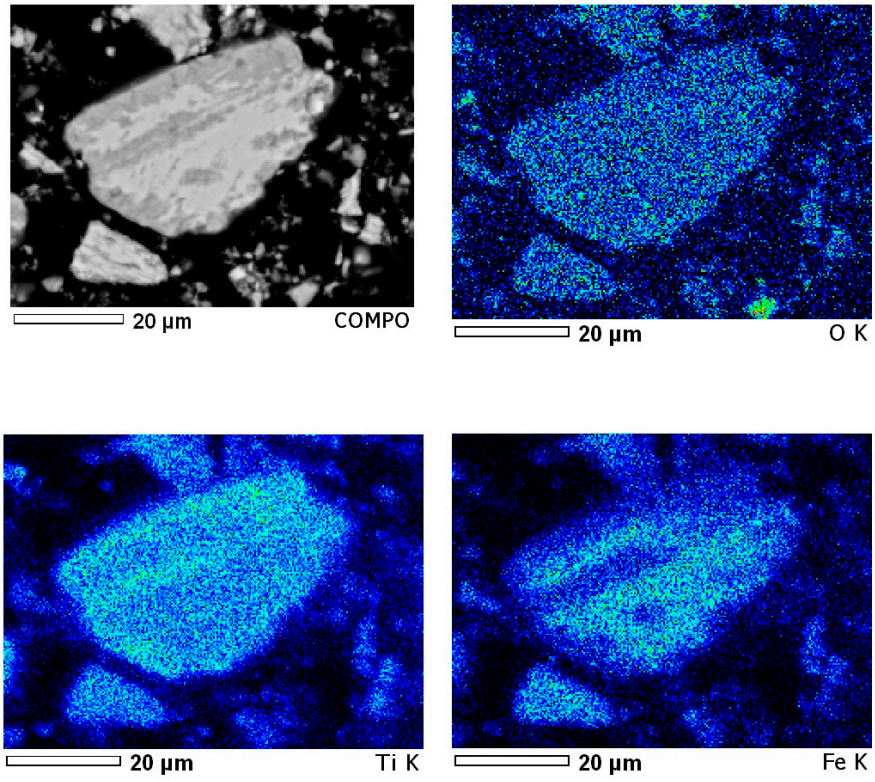

Figure 3. SEM-EDS elemental mapping of ilmenite concentrate.

Rutile and ilmenite were present in the first sample of the ilmenite concentrate in this mineralogical study. Rutile (TiO_2) is a light grey mineral of low reflectivity. Its internal reflections are of thick brown with a reddish tint. The mineral is anisotropic and anhedrally shaped (Figure 4).

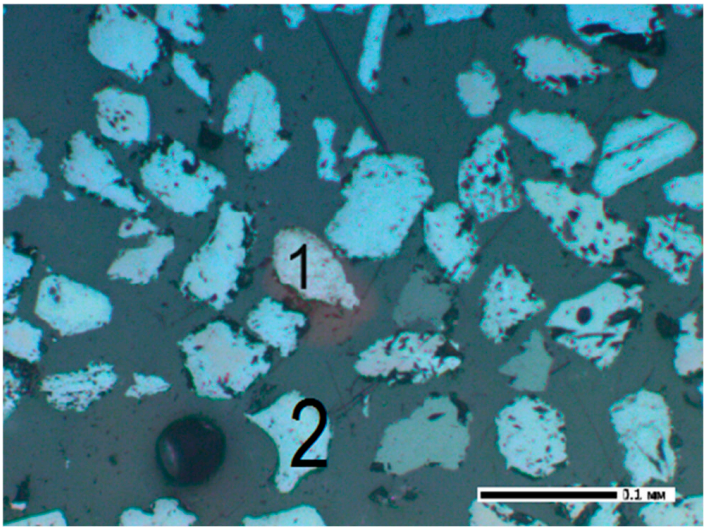

Figure 4. Rutile (1) and ilmenite (2). Sample No. 1, ×200.

The oxidative roasting of ilmenites is performed to oxidase the divalent iron to Fe_2O_3 and Fe_3O_4, to achieve the further direct reduction of iron during smelting, and for the conversion of chromites into magnetic fractions for the electrostatic separation of chromites from titanium-containing fractions.

Oxidative roasting oxidizes FeO into Fe_2O_3 through the following reaction:

$$2FeTiO_3 + 1/2O_2 = Fe_2O_3 + 2TiO_2. \quad (2)$$

Oxidative roasting with ilmenite of the Obukhovskoye deposit was performed at 900, 1000, and 1100 °C, without the addition of soda and also with the addition of 4% and 6% soda. The results of one series of oxidative roasting experiments are presented in Table 6.

The yield of the non-magnetic fraction was small and ranged from 11.3% to 10.0%. However, the extraction of titanium into the magnetic fraction was much higher than into the non-magnetic fraction. The extraction of iron into the magnetic fraction was 86.5% to 92.8%, and there was almost no reduced metallic iron. According to the X-ray phase analysis (Figure 5), the crystalline phase was detected in the magnetic fraction at 900 °C without the soda, comprising mainly ilmenite $Fe_{1.04}Ti_{0.96}O_3$ and rutile, syn. $Ti_{0.992}O_2$.

X-ray phase analysis of the magnetic fraction with 4% soda (Figure 5) shows the presence of a new phase, freudenbergite, syn. $Na_2(Fe_2Ti_6O_{16})$, as it appears due to the interaction of soda with ilmenite. The presence of ilmenite and rutile in fairly large quantities in the magnetic fractions of roasting at a temperature of 900 °C without the addition of soda ash and with 4% soda ash shows the insufficient reduction of iron and the transition of titanium to a non-magnetic fraction.

The second series of experiments was carried out at a temperature of 1000 °C. The furnace mode remained similar to that used in the first series of experiments. The results of the oxidative roasting experiments at a temperature of 1000 °C are presented in Table 7.

According to the results of Table 7, the yield of the non-magnetic slag fraction increased from 9.7% to 19.3%, and the extraction of titanium into the slag fraction increased markedly from 8.4% to 18.9%. The extraction of titanium into the magnetic fraction also remained high and varied from 91.6% to 81.1%. It was confirmed by X-ray phase analysis (Figure 6) that in the magnetic fraction at a temperature of 1000 °C, without soda ash, the phase of

ilmenite $Fe_{1.04}Ti_{0.96}O_3$ decreased and amounted to 59.9%, while the phase of rutile syn. $Ti_{0.992}O_2$, increased to 31.9%.

Table 6. Results of oxidative roasting experiments at 900 °C.

Name of the Product	Exit, %	TiO_2		Fe_{total}		Cr_2O_3	
		Content, %	ε, %	Content, %	ε, %	Content, %	ε, %
Temperature, 900 °C, without soda							
Briquettes (charge)	100	50.5	100	16.59	100	3.36	100
Cinder	81.87	61.7	100	20.26	100	4.1	100
Magnetic fraction	88.7	69.44	99.8	2.75	86.5	4.43	95.8
Non-magnetic fraction	11.3	55.48	0.2	24.1	13.5	1.51	4.2
Total:	100		100		100		100
Temperature, 900 °C, 4% soda							
Briquettes (charge)	100	48.04	100	15.77	100	3.2	100
Cinder	76.8	62.55	100	20.53	100	4.2	100
Magnetic fraction	90.8	46.11	92.02	19.9	88.0	4.4	96.3
Non-magnetic fraction	9.2	54.2	7.98	25.0	12,0	1.67	3.7
Total:	100		100		100		100
Temperature, 900 °C, 6% soda							
Briquettes (charge)	100	46.81	100	15.36	100	3.11	100
Cinder	74.7	62.7	100	20.57	100	4.17	100
Magnetic fraction	90.0	63.5	91.2	20.0	92.8	4.5	96.0
Non-magnetic fraction	10.0	55.0	8.8	25.6	7.2	1.65	4.0
Total:	100		100		100		100

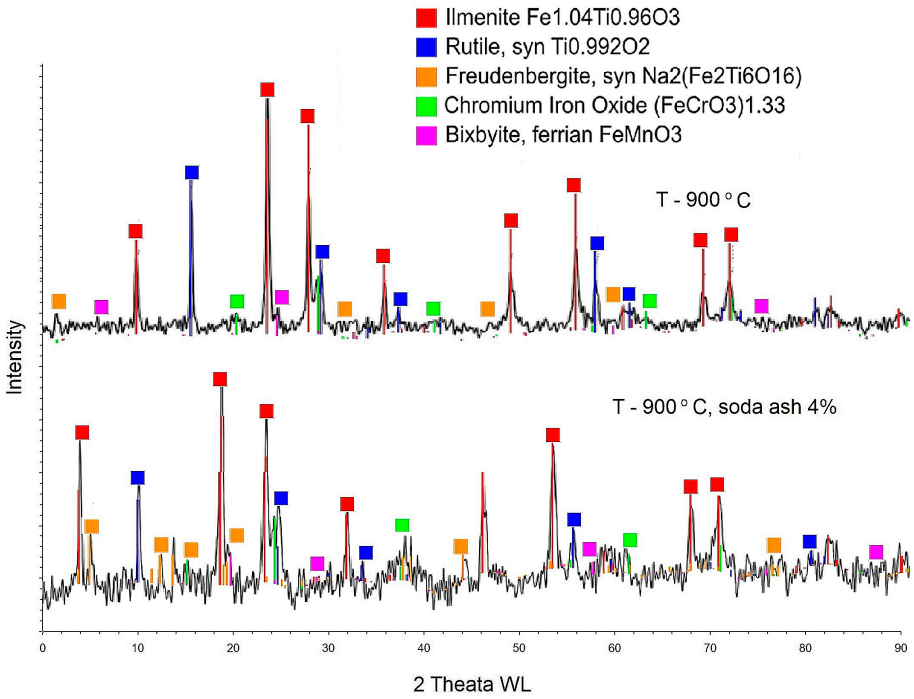

Figure 5. X-ray diffraction pattern of magnetic fraction at 900 °C.

Table 7. Results of oxidizing experiments at 1000 °C.

Name of the Product	Exit, %	TiO_2		Fe_{total}		Cr_2O_3	
		Content, %	ε, %	Content, %	ε, %	Content, %	ε, %
Temperature, 1000 °C, without soda							
Briquettes (charge)	100	50.5	100	16.58	100	3.36	100
Cinder	79.1	63.85	100	20.96	100	4.25	100
Magnetic fraction	90.3	64.8	91.6	21.5	92.8	4.51	96.0
Non-magnetic fraction	9.7	55.4	8.4	15.6	7.2	1.75	4.0
Total:	100		100		100		100
Temperature, 1000 °C, 4% soda							
Briquettes (charge)	100	48.04	100	15.77	100	3.2	100
Cinder	90.96	52.8	100	17.33	100	3.51	100
Magnetic fraction	90.0	52.17	89.0	17.49	90.7	3.73	95.7
Non-magnetic fraction	10.0	58.5	11.0	15.9	9.3	1.5	4.3
Total:	100		100		100		100
Temperature, 1000 °C, 6% soda							
Briquettes (charge)	100	46.8	100	15.4	100	3.1	100
Cinder	78.48	59.6	100	19.6	100	3.96	100
Magnetic fraction	80.7	60.0	81.1	20.4	84.0	4.57	93.1
Non-magnetic fraction	19.3	58.2	18.9	16.1	16.0	1.42	6.9
Total:	100		100		100		100

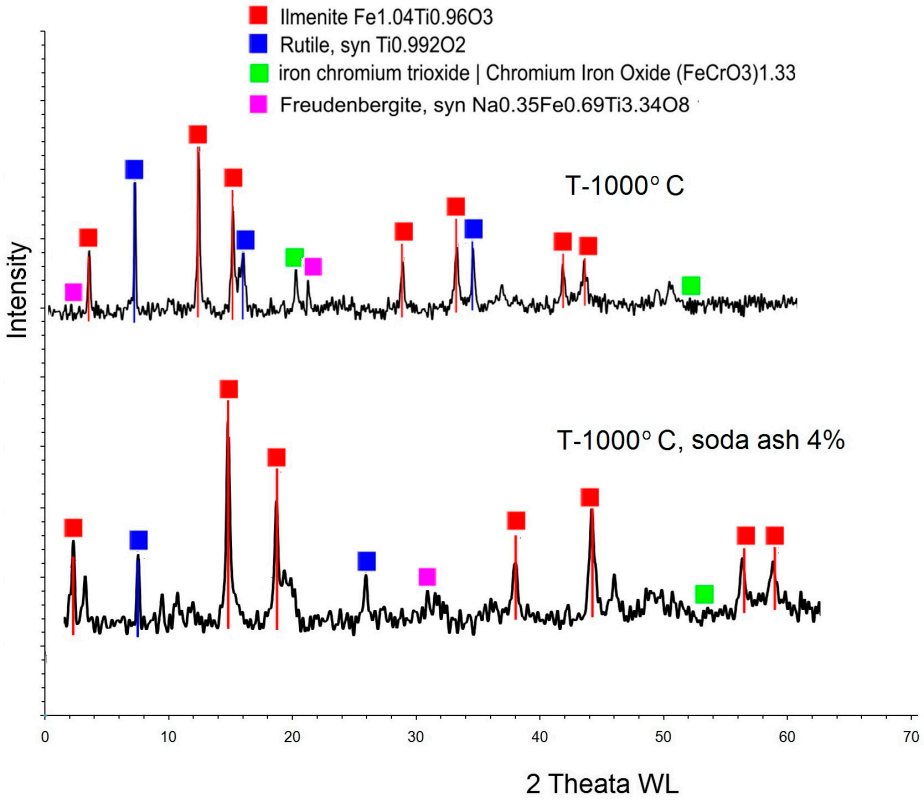

Figure 6. X-ray diffraction pattern of the magnetic fraction at 1000 °C.

X-ray phase analysis of the magnetic fraction at 1000 °C with 4% soda (Figure 6) shows an increase in the ilmenite phase (63.4%), a decrease in the rutile phase (16.3%), and an increase in a new phase of freudenbergite syn. $Na_2(Fe_2Ti_6O_{16})$ phase (11.9%) at the expense of a greater quantity of soda addition. The extraction of iron into the non-magnetic fraction at 1000 °C increased from 7.2 to 16%, and the extraction of chromium into the non-magnetic fraction also increased from 4.0 to 6.9%.

The third series of roastings was conducted at 1100 °C, and the furnace mode was similar to that used in the first series of experiments. Table 8 shows the results of the oxidative roasting experiments at 1100 °C.

Table 8. Results of oxidizing experiments at 1100 °C.

Name of the Product	Exit, %	TiO_2		Fe_{total}		Cr_2O_3	
		Content, %	ε, %	Content, %	ε, %	Content, %	ε, %
Temperature, 1100 °C, without soda							
Briquettes (charge)	100	50.5	100	16.57	100	3.36	100
Cinder	75.2	67.2	100	22.05	100	4.47	100
Magnetic fraction	85.3	68.9	87.0	20.8	80.3	5.07	96.8
Non-magnetic fraction	14.7	57.4	13.0	29.5	19.7	1.0	3.2
Total:	100		100		100		100
Temperature, 1100 °C, 4% soda							
Briquettes (charge)	100	48.05	100	15.77	100	3.2	100
Cinder	80.92	59.4	100	19.5	100	3.95	100
Magnetic fraction	87.6	59.8	88.2	20.2	90.9	4.3	95.8
Non-magnetic fraction	12.4	56.6	11.8	14.3	9.1	1.3	4.2
Total:	100		100		100		100
Temperature, 1100 °C, 6% soda							
Briquettes (charge)	100	46.81	100	15.36	100	3.11	100
Cinder	71.36	65.6	100	21.5	100	4.36	100
Magnetic fraction	96.4	66.1	97.3	21.86	97.9	4.5	99.0
Non-magnetic fraction	3.6	50.0	2.7	12.3	2.1	1.2	1.0
Total:	100		100		100		100

According to the oxidative roasting results (Table 8), the extraction of titanium into the magnetic fraction increased from 87.0% to 97.3%. There was very little metallic reduced iron—a few coagulated small metallic droplets.

According to the X-ray phase analysis (Figure 7), the crystalline phase detected in the magnetic fraction at 900 °C without soda was mainly rutile (47.9%) and ilmenite (14.7%). It is worth noting that the XRD analysis identified new phases, i.e., iron manganate Fe_2MnO_4 (12.0%), metallic iron (11.3%), and iron titanium oxide $Fe_{1.69}Ti_{0.22}O_3$ (9.9%). That is, as the phase composition of the magnetic fraction changed, reduced iron appeared, and the ilmenite was gradually reduced to iron, with the transition of titanium to the oxide form with increases in temperature.

X-ray phase analysis of the magnetic fraction with 4% soda at a temperature of 1100 °C is shown in Figure 7. It indicates the appearance of new phases such as freudenbergite syn. $Na_2(Fe_2Ti_6O_{16})$ (9.6%), magnetite (17.0%), and ferrous bixbyite $FeMnO_3$ (7.1%) due to the presence of soda.

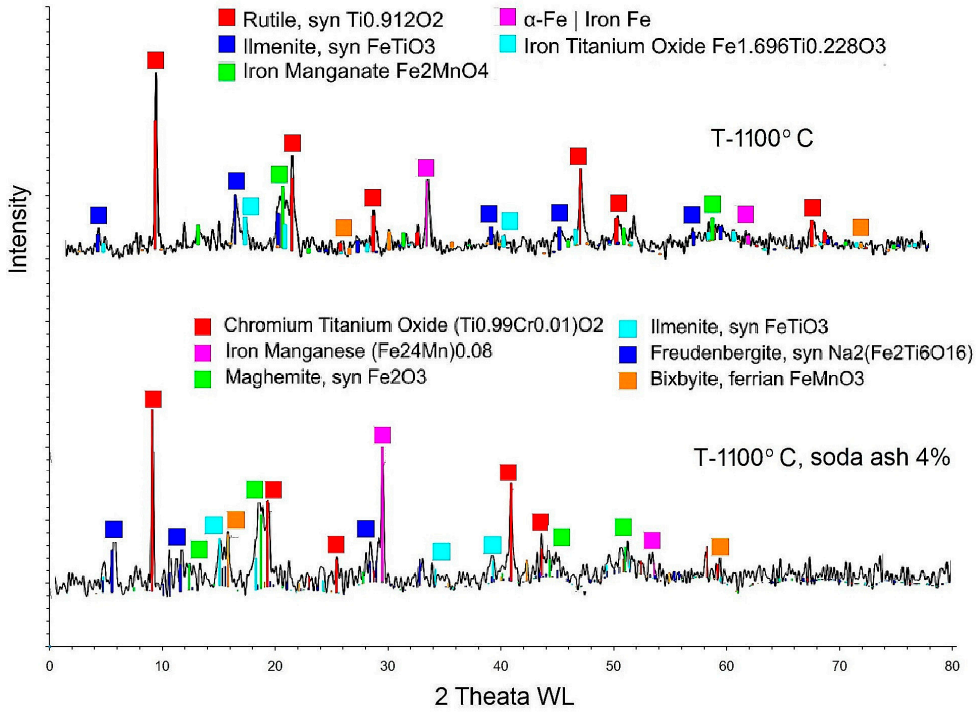

Figure 7. X-ray diffraction pattern of the magnetic fraction at 1100 °C.

According to the results of the X-ray phase analysis of the magnetic fraction, more rutile and unchanged ilmenite phases were formed after roasting the ilmenite concentrate without the addition of soda, and the rutile phase became slightly larger than the ilmenite phase with increases in the roasting temperature. A new phase of freudenbergite syn., appeared in the magnetic fraction after roasting when soda was added.

The optimal parameters of the oxidative roasting were as follows: a temperature of 1000 °C with the addition of 6% calcined soda. Under these conditions, the yield of the non-magnetic fraction was the highest, amounting to 19.3%. The extraction of titanium into the non-magnetic fraction was also the highest, amounting to 18.9%. However, the extraction of titanium into the magnetic fraction was greater than that into the non-magnetic fraction, and the loss of titanium with the magnetic fraction was noticeable.

3.2. Reducing Roasting of Ilmenite Concentrate

Since the metallic iron and non-magnetic fractions were insufficient during oxidative roasting, it was decided to conduct reducing roasting of the ilmenite concentrate. The temperature for the reducing roasting was chosen by taking into account the optimal temperature of 1000 °C for oxidative roasting. The roasting was performed without the addition of soda and also with the addition of 4% and 6% soda. The charge was made in the same way as for the oxidative roasting. The furnace mode was as follows: the briquettes were heated in the furnace up to 1000 °C for 100 min and were then kept for 30 min at the set temperature, followed by cooling to 700 °C in argon medium. The results of the reducing roasting experiments at 1000 °C are presented in Table 9.

According to Table 9, the extraction of titanium into the magnetic fraction was less than that into the oxidative roasting and varied from 60.3% to 65.5%. The extraction of iron into the magnetic fraction varied from 74.1% to 86.4%, and the extraction of chromium varied from 75.1 to 91.0%.

Table 9. Results of experiments of reducing roasting at 1000 °C.

Name of the Product	Exit, %	TiO_2		Fe_{total}		Cr_2O_3	
		Content, %	ε, %	Content, %	ε, %	Content, %	ε, %
Temperature, 1000 °C, without soda							
Briquettes (charge)	100	50.5	100	16.58	100	3.36	100
Cinder	94.1	53.65	100	17.61	100	3.57	100
Magnetic fraction	64.14	50.4	60.3	23.4	85.1	4.3	77.2
Non-magnetic fraction	35.86	59.5	39.7	7.3	14.9	2.3	22.8
Total:	100		100		100		100
Temperature, 1000 °C, 4% soda							
Briquettes (charge)	100	48.05	100	15.8	100	3.2	100
Cinder	93.36	51.5	100	16.9	100	3.4	100
Magnetic fraction	69.9	48.3	65.5	17.9	74.1	3.7	75.1
Non-magnetic fraction	30.1	58.9	34.5	14.5	25.9	2.8	24.9
Total:	100		100		100		100
Temperature, 1000 °C, 6% soda							
Briquettes (charge)	100	46.8	100	23.86	100	3.1	100
Cinder	93.8	49.9	100	25.4	100	3.3	100
Magnetic fraction	69.68	46.7	65.2	31.55	86.4	4.3	91.0
Non-magnetic fraction	30.32	57.3	34.8	11.41	13.6	0.98	9.0
Total:	100		100		100		100

The XRD spectra of the magnetic fraction without soda ash and with 4% soda ash and 6% soda ash at 1000 °C are shown in Figure 8. X-ray diffraction analysis of the 1000 °C magnetic fraction without soda shows the following phases: rutile (68.9%), ilmenite (14.4%), hematite (12.2%), and iron–aluminochromite silica $(Fe_{2.81}Cr_{0.15})(A_{l0.4}0_2Si_{0.598})$ (4.5%). For the initial charge without soda, the presence of ilmenite and rutile indicates that the destruction of the ilmenite was not complete, the iron did not recover into the metal, and the titanium remained in the magnetic fraction. X-ray analysis of the magnetic fraction at 1000 °C with 4% soda shows the following phases: freudenbergite $Na_2(Fe_2Ti_6O_{16})$ (58.8%), ilmenite (22.2%), chromite $(Fe_{0.976}Al_{0.023})(Fe_{0.023}Al_{0.329}Cr_{1.647})O_4$ (10.4%), and iron–aluminochromite silicon $(Fe_{2.81}Cr_{0.15})(Al_{0.4}0_2Si_{0.598})$ (8.6%). X-ray analysis of the magnetic fraction at 1000 °C with 6% soda shows the following phases: rutile (53.7%), ilmenite (27.1%), hematite (12.2%), and iron–aluminochromite silica $(Fe_{2.81}Cr_{0.15})(A_{l0.4}0_2Si_{0.598})$ (7.0%).

The XRD spectra of the non-magnetic fraction without soda ash and with 4% and 6% soda ash at 1000 °C are shown in Figure 9. The phases of the non-magnetic fraction at 1000 °C without soda were as follows: rutile (49.7%), magnesian chromite $(Fe_{0.50}Mg_{0.50})(Cr_{0.71}A_{l0.29})_2O_4$ (20.4%), ilmenite (14.7%), hematite (10.6%), and quartz (4.6%). The phases of the non-magnetic fraction at 1000 °C with 4% soda were as follows: freudenbergite $Na_2(Fe_2Ti_6O_{16})$ (45.9%), magnesian chromite $(Fe_{0.50}Mg_{0.50})(Cr_{0.71}Al_{0.29})_2O_4$ (18.3%), and ilmenite (35.8%). The phases of the non-magnetic fraction at 1000 °C with 6% soda were as follows: rutile (43.6%), ilmenite (33.5%), magnesian chromite $(Fe_{0.50}Mg_{0.48})(Cr_{0.72}Al_{0.28})_2O_4$ (15.3%), and quartz (7.6%). Chromite phases were found in both the magnetic and non-magnetic fractions during the reduction, as well as when soda was added.

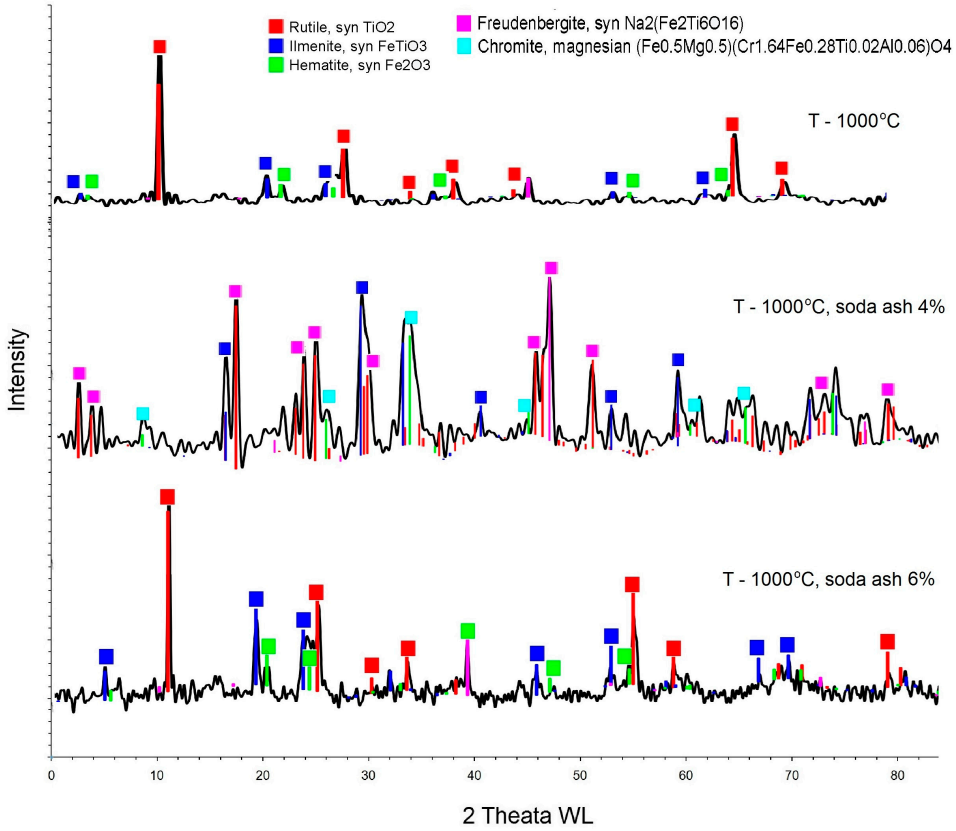

Figure 8. X-ray diffraction pattern of the magnetic fraction at 1000 °C.

The optimal parameters of the reduction roasting were as follows: a temperature of 1000 °C; 6% soda was added to the charge; the sinter yield from the original material was 93.8%. The yield of the magnetic fraction was 69.68%, and the yield of the non-magnetic fraction was 30.32%. The extraction of titanium into the magnetic fraction was 65.2%, that of iron was 86.4%, that of chromium was 91.0%, and that of the ΣREE (rare-earth elements) was 90%. The extraction of titanium into the non-magnetic fraction was 34.8%, that of iron was 13.6%, that of chromium was 9.0%, and that of the ΣREE was 10%.

The reduction of iron oxides from the ilmenite occurs in the presence of carbon at temperatures above 800 °C, according to the following equations:

$$FeO{\cdot}TiO_2 + C = Fe + TiO_2 + CO, \quad (3)$$

$$FeO{\cdot}TiO_2 + CO = Fe + TiO_2 + CO_2 \quad (4)$$

The reduction of chromite proceeds according to the following reaction:

$$FeO{\cdot}Cr_2O_3 + C = Cr_2O_3 + Fe + CO \quad (5)$$

A polished section of sample No. 1 from the magnetic fraction of the reducing roasting at 1000 °C without the addition of soda was analyzed. Reduced metallic iron was found along the edges of the ilmenite particles in magnetic fraction No. 1 (Figure 10).

Figure 11 shows an image of sample No. 2, with a particle of the magnetic fraction which was not decomposed by reducing roasting (1000 °C) without soda, where areas of manganous ilmenite, ilmenite with chromium admixture, rutile, and ilmenite can be observed. The image of sample No. 3 (roasting temperature of 1000 °C, without soda) of the non-magnetic fraction is shown in Figure 12. The maximum number of mineral particles in the heavy fraction found in the sample was more than that in the magnetic fraction (monazite and columbite).

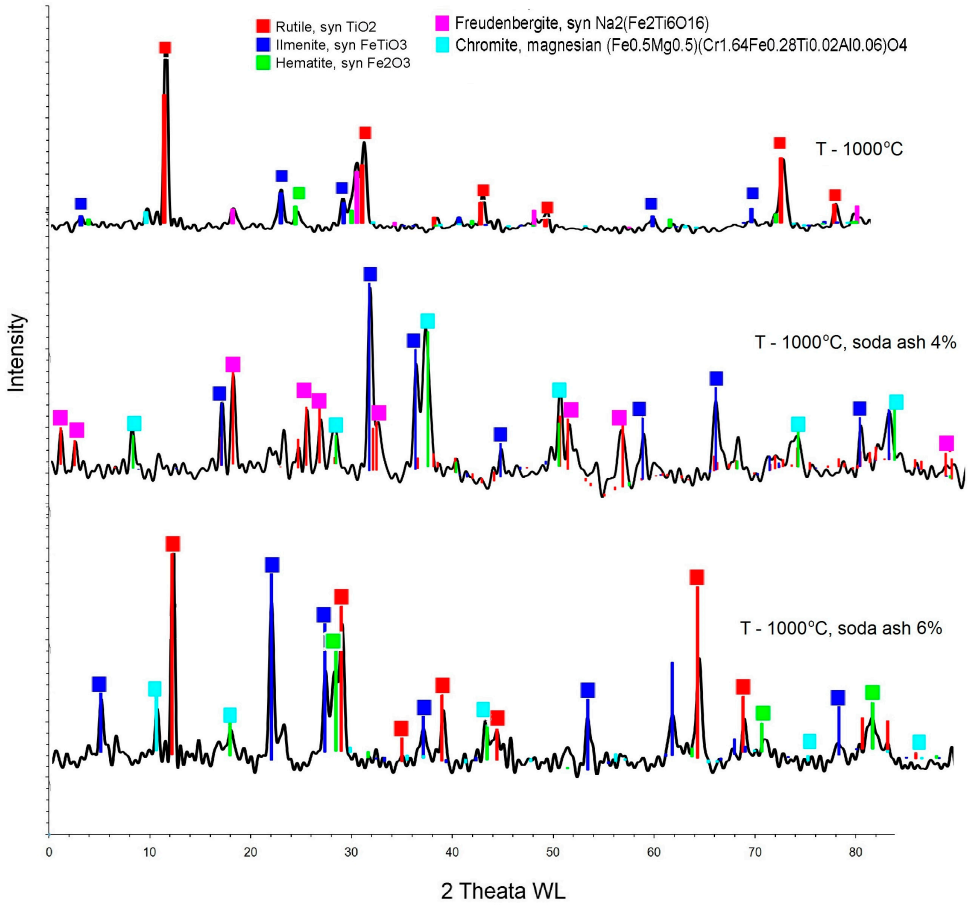

Figure 9. X-ray diffraction pattern of non-magnetic fraction at 1000 °C.

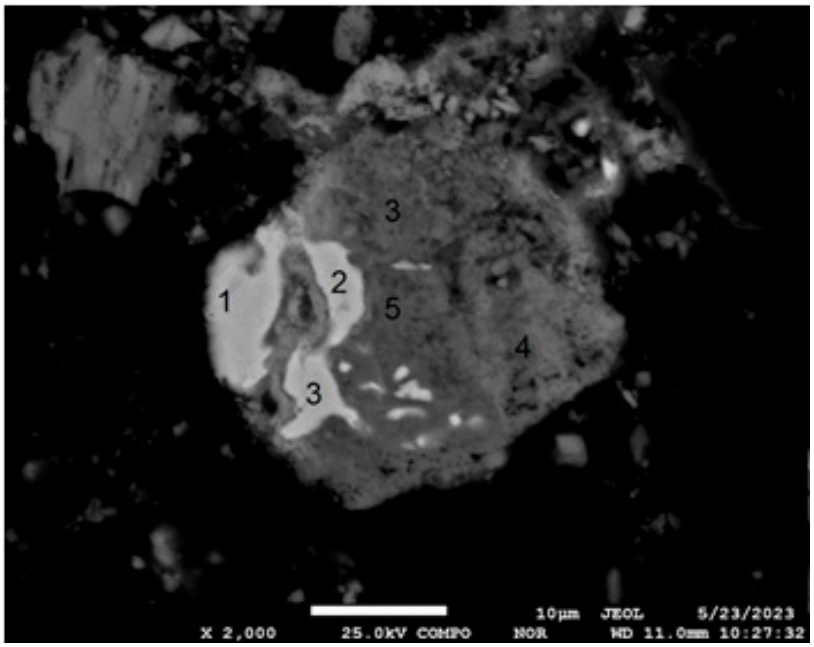

Figure 10. Image of sample No. 1 of the magnetic fraction, showing ilmenite particles with locations of reduced iron (1), ilmenite (2,3,5), and manganous ilmenite (4). COMPO mode, ×2000.

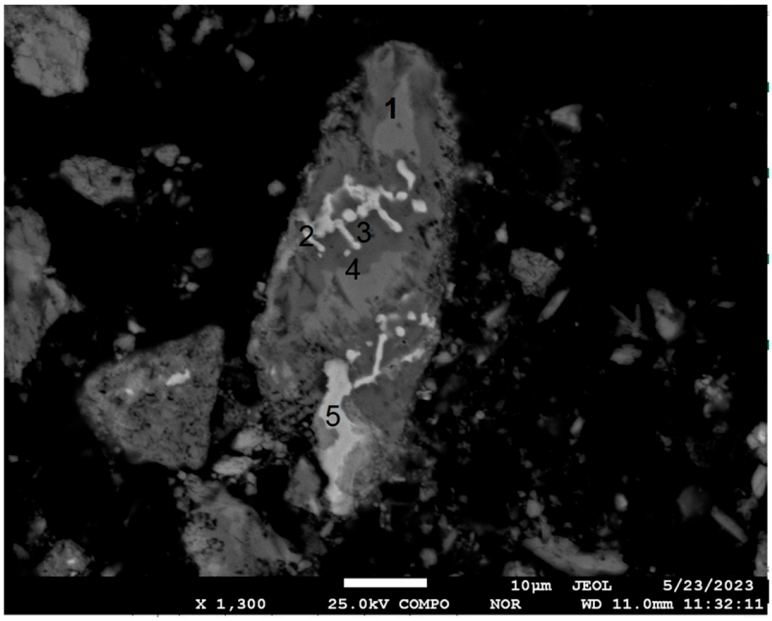

Figure 11. Image of sample No. 2 of the magnetic fraction, showing ilmenite particles with localizations of manganous ilmenite (1,4), ilmenite with chromium admixture (2), rutile (3), and ilmenite (5). COMPO mode, ×1300.

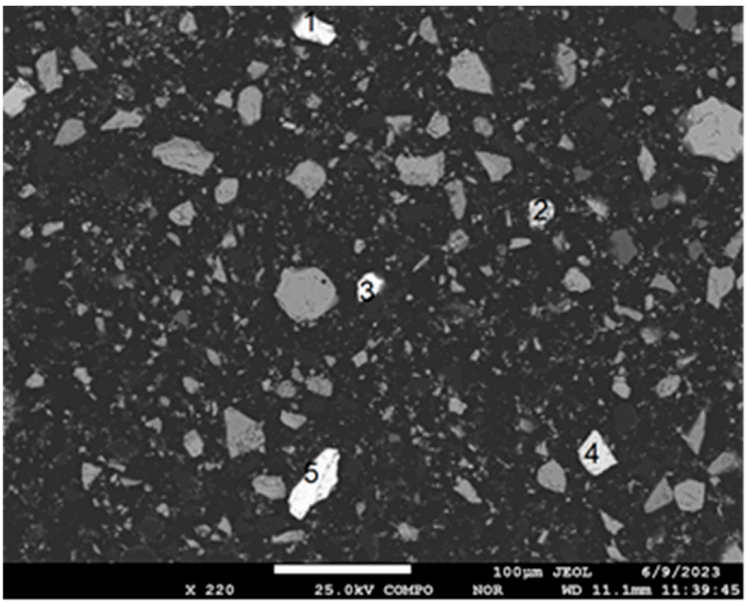

Figure 12. Image of sample No. 3 of the non-magnetic fraction, showing monazite particles (1,2,3,5) and columbite particles (4). COMPO mode, ×220.

Electron probe studies were carried out with the polished section of sample No. 4 of the magnetic fraction obtained from the sinter of the reducing roasting at 1000 °C with the addition of 4% soda (Figure 13). Monazite and soda inclusions with monazite were found in the studied sample at ×1600 magnification. The sodium layer of monazite with sodium inclusions (2) contained fewer particles of heavy fraction than in monazite (1). Moreover, sodium follows channels, sometimes bypassing more resistant compounds. The particles of undecomposed ilmenite on the titanium oxide and reduced metallic iron are shown, which is why there are chrome spinelides embedded in the ilmenite lattice. The interaction of monazite with soda shows the partial disintegration of the monazite crystal at the boundaries

of soda disintegration, which was confirmed by SEM-EDS elemental mapping, as shown in Figure 14. Presumably, this indicates either a lack of soda or a low temperature.

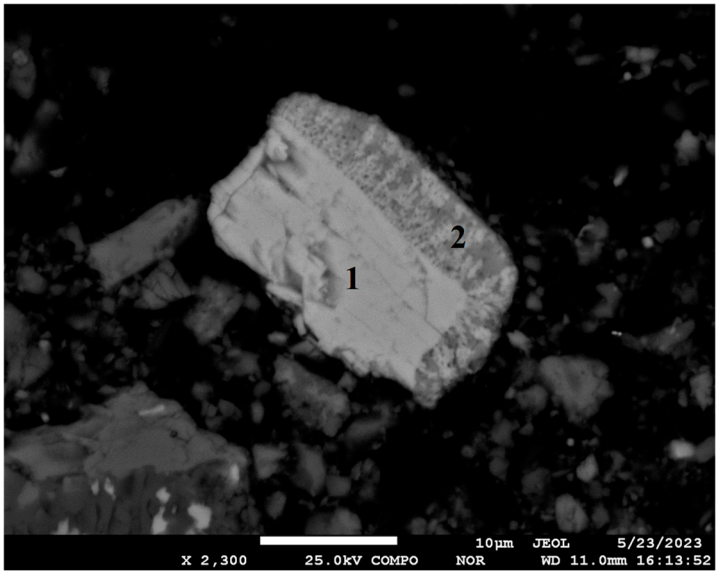

Figure 13. Image of sample No. 3 of the magnetic fraction, showing monazite (1) and monazite with sodium inclusions (2). COMPO mode, ×2300.

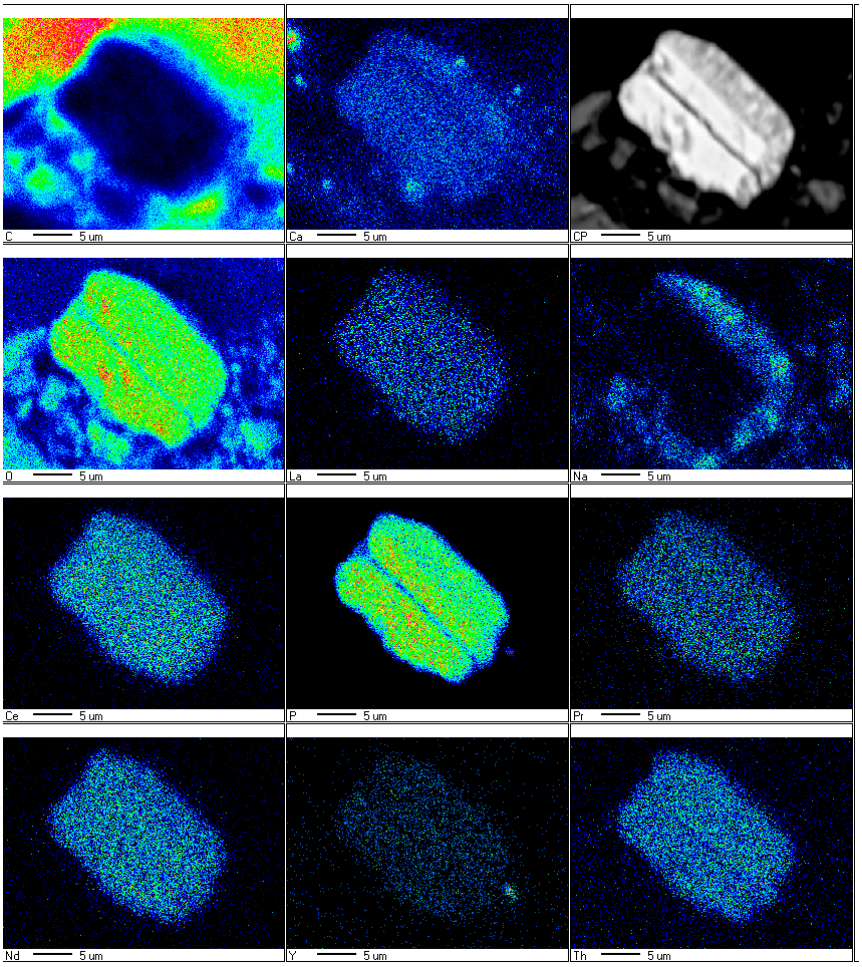

Figure 14. SEM-EDS elemental mapping of the magnetic fraction.

The image of sample No. 5 of the non-magnetic fraction with the addition of 4% soda ash (Figure 15) shows ilmenite particles with increased titanium content and a chromium admixture, which is supported by the SEM-EDS elemental mapping (Figure 16).

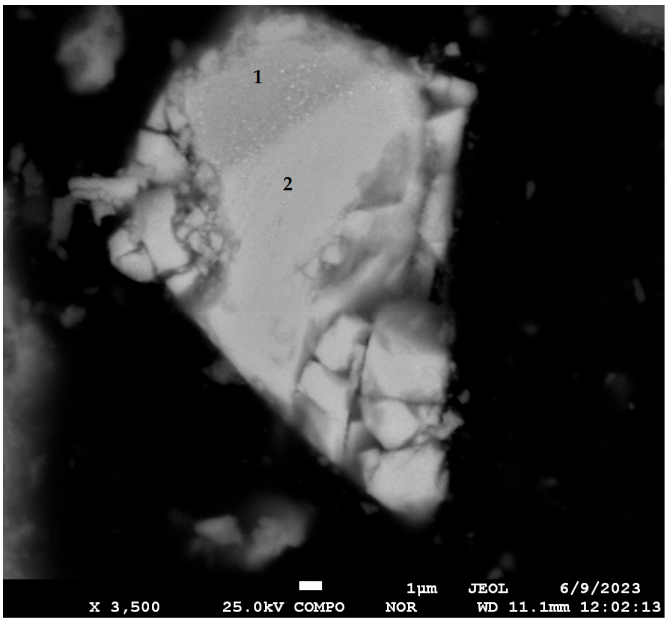

Figure 15. Image of sample No. 5 of the non-magnetic fraction, showing particles of ilmenorutile with an admixture of chromium (1) and ilmenite (2). COMPO mode, ×3500.

Conclusions can be drawn, based on the mineralogical compositions of the investigated samples. Ilmenite, chromium spinelides, and rutile were found in the magnetic fraction of the sinter of the reducing roasting at 1000 °C without soda. The ilmenite concentrate minerals did not decompose into reduced iron and a slag fraction containing titanium oxides. Reduced iron occurred only at the edges of the ilmenite, and the partial reduction of the iron occurred in the chromium spinelides, ilmenorutile, and the ilmenite itself, so they remained in the magnetic fraction.

Ilmenite, chromium spinelides, monazite, and xenotime were contained in the non-magnetic fraction from the same reducing roasting experiment without soda. The content of chromium spinelides with the released iron during the reduction process in the non-magnetic fraction is explained by the fact that chromium spinel is non-magnetic. The discovery of rare-earth minerals in the non-magnetic fraction in the form of monazite and xenotime confirms their concentration.

Chromium-spinel, ilmenite, monazite, and xenotime were found in the second magnetic fraction in the same way as in the first magnetic fraction. A new phase, freudenbergite $Na_2(Fe_2Ti_6O_{16})$, appeared wherever the sodium interacted with the ilmenite. The interaction of soda with ilmenite, as well as with monazite, is visible in the electron probe microscope photographs. Moreover, the destruction of the crystal lattice, or the activation of the lattice of rare-earth phosphates, is clearly demonstrated in Figure 13.

Thus, no reduced metallic iron was formed during the reducing roasting process; up to 65.2% of the titanium was lost with the magnetic fraction. The slag fraction was low in titanium and had a high iron content, as 34.8% titanium and 13.6% iron were extracted into the non-magnetic fraction. In this regard, an experiment was performed to smelt the ilmenite concentrate.

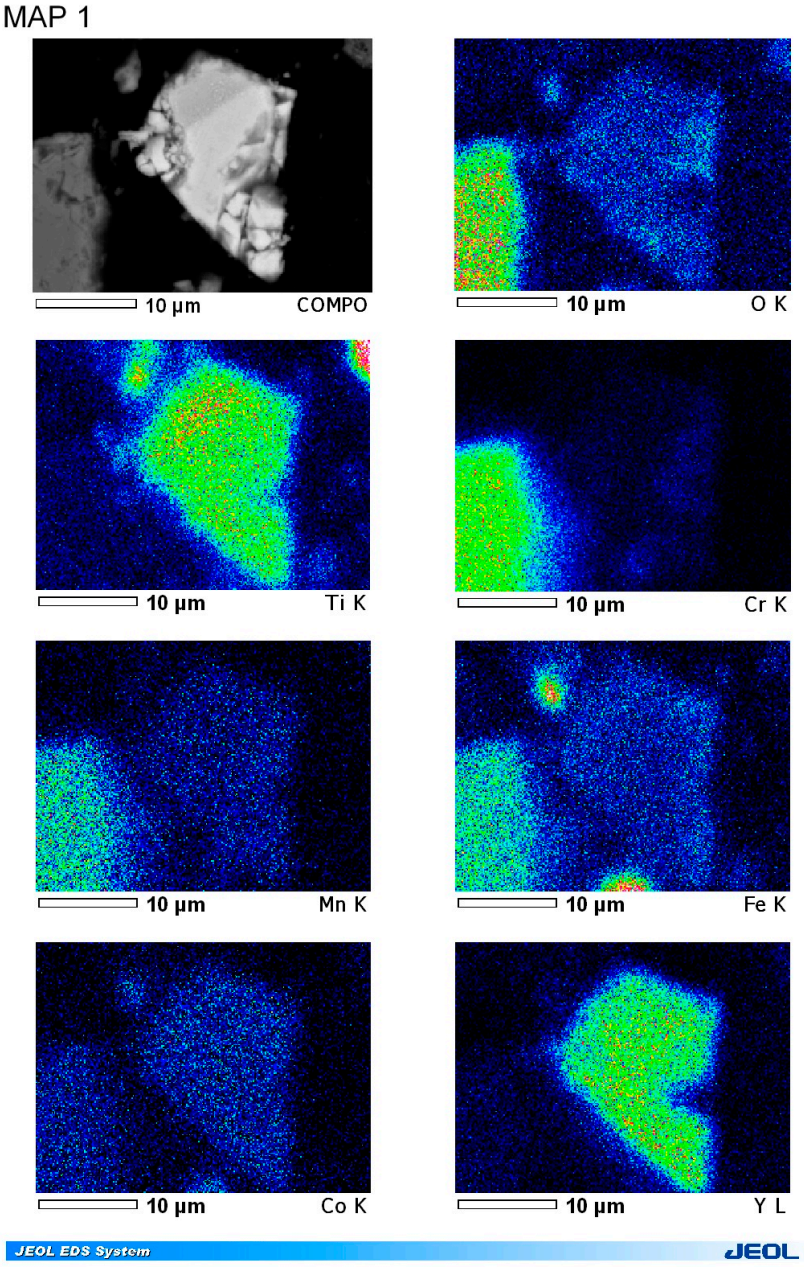

Figure 16. SEM-EDS elemental mapping of the non-magnetic fraction.

3.3. Smelting Process of Ilmenite Concentrate with High Chromium Content

The technology of solid-phase carbothermic reduction and the liquid-phase reduction smelting of titanium-containing concentrates in electric furnaces for the preliminary separation of iron into an independent phase has become quite widely used in the titanium sub-industry. Electric smelting is rational and represents the most effective way to separate iron from titanium dioxide compared to other methods used to process titanium raw materials. In this case, two commercial products were obtained, in the form of titanium slag with 70–90% TiO_2 and cast iron alloyed with titanium, vanadium, and chromium.

The total reduction process of ilmenite can be represented by the following equation:

$$Fe_2O_3 \cdot TiO_2 \rightarrow Fe_3O_4 \cdot TiO_2 \rightarrow FeO \cdot TiO_2 \rightarrow Fe + TiO_2 \quad (6)$$

Titanium dioxide is also reduced through several intermediate compounds:

$$TiO_2 \rightarrow Ti_2O_5 \rightarrow Ti_2O_3 \rightarrow TiO \rightarrow TiC \quad (7)$$

Hematite is reduced according to the following scheme:

$$Fe_2O_3 \rightarrow Fe_3O^4 \rightarrow FeO \rightarrow Fe \quad (8)$$

Two-stage smelting was carried out in a tubular, vertical furnace. The mixed charge was poured into a graphite crucible.

X-ray diffraction analysis of the initial charge (Figure 17) shows the following phases: iron (III) titanium oxide phase (Fe_2TiO_5) (30.0%), ilmenite ($Fe_{1.04}Ti_{0.96}O_3$) (26.1%), rutile (TiO_2) (21.2%), iron oxide (Fe_2O_3) (12.4%), and iron–chromium oxide hydroxide $Fe(CrO_4)$ (10.2%).

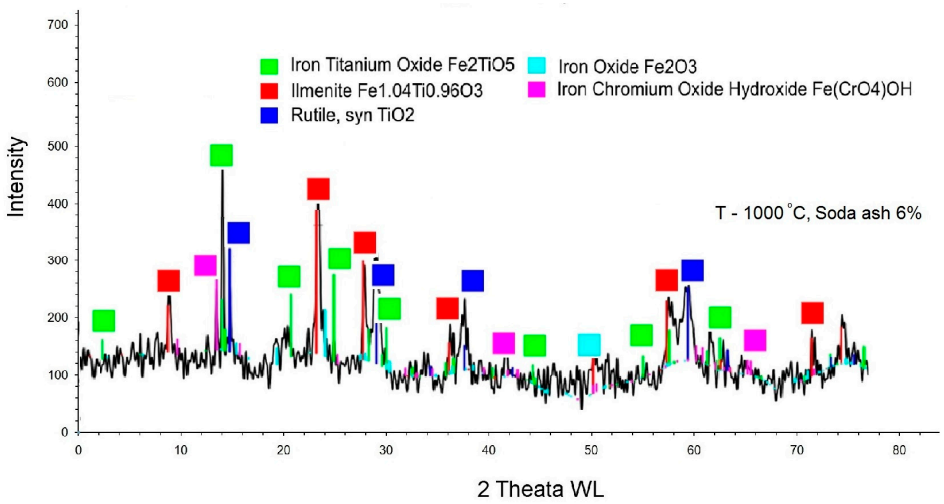

Figure 17. X-ray diffraction pattern of the initial charge.

The sinter was crushed and magnetic separation was performed at a magnetic field strength of 180 Oersted. Table 10 presents the results of the reduction smelting and magnetic separation of the sinter.

Table 10. Results of reduction smelting and the magnetic separation of cinder.

Name of the Product	Exit, %	TiO_2		Fe_{total}		Cr_2O_3		ΣREE	
		Content, %	ε, %	Content, %	ε, %	Content, %	ε, %	Content, %	ε, %
Charge	100	47.4	100	15.57	100	3.2	100	0.46	100
Cinder	69.3	68.5	100	22.5	100	4.56	100	0.66	100
Magnetic fraction	43.0	67.6	78.4	26.1	92.1	5.22	91.0	0.43	28.0
Non-magnetic fraction	57.0	71.96	21.6	8.65	7.9	1.99	9.0	0.84	72.0
Total:	100		100		100		100		100

The second smelting was performed in a single stage at 1600 °C in a Kejia chamber furnace in an argon environment. Seven briquettes measuring 16 × 19 mm were made and then placed in a graphite crucible. The charge consisted of 87.6% ilmenite concentrate, 2.6% soda ash, 8.8% coke, and 1% molasses. The second smelting results are presented in Table 11.

Table 11. Results of the reduction smelting and magnetic separation of cinder.

Name of the Product	Exit, %	TiO_2		Fe_{total}		Cr_2O_3	
		Content, %	ε, %	Content, %	ε, %	Content, %	ε, %
Briquette (charge)	100	53.95	100	17.71	100	3.6	100
Cinder	77.85	69.3	100	22.75	100	4.61	100
Magnetic fraction	80.5	65.45	76.0	25.99	92.0	3.71	90.5
Non-magnetic fraction	19.5	85.04	24.0	9.34	8.0	2.25	9.5
Total:	100		100		100		100

The extraction of total iron into the magnetic fraction was 92%; no metallic iron was found. The extraction of titanium oxide into the non-magnetic fraction was small, amounting to 24%, and that into the magnetic fraction was 76%; there was no separation into the slag and reduced iron metal, which was probably due to the small amount of soda.

For the third reduction smelting, a 35 × 20 mm briquette was made and then placed in a corundum crucible. The reduction smelting mode was as follows: the temperature was raised to 1700 °C over a period of 170 min, where it was held for 30 min in an argon environment. The sinter yield was 85.23%. During the smelting process, an alloy was obtained in the form of a reduced iron ingot weighing 25.78 g, as shown in the photograph in Figure 18.

Figure 18. Iron alloy obtained by smelting at 1700 °C.

The sinter was crushed and magnetic separation was performed. The yield of the magnetic fraction was 60.0%, and the yield of the non-magnetic fraction was 40.0%. The extraction of metallic iron into the magnetic fraction was 43.16%, and that of iron in the form of Fe_2O_3 oxide was 46.95%. The extraction of titanium oxide into the non-magnetic fraction was 49.2%, that of iron oxide was 9.89%, and that of chromium oxide was 10%. Table 12 shows the results of reduction smelting at 1700 °C.

The optimal conditions for the reduction smelting were determined to be at 1700 °C with the addition of 6% soda. The single-stage smelting mode of the ilmenite concentrate was as follows: the temperature was raised to 1700 °C, with a heating step of 10 °C/min with argon supply, and then held for 30 min, followed by cooling to 700 °C in an argon environment.

During the smelting, the extraction of titanium into the non-magnetic fraction was higher, at 49.2%, than in the first and second smeltings. The iron was formed into a metal ingot of reduced metal. Moreover, during smelting, up to 68–72% of the REE passed into the non-magnetic fraction.

Table 12. Results of reduction smelting at 1700 °C.

Name of the Product	Exit, %	TiO_2		Fe_{total}		Fe_{metall}	Cr_2O_3		ΣREE	
		Content., %	ε, %	Content., %	ε, %	Content., %	Content., %	ε, %	Content., %	ε, %
Briquette (charge)	100	55.52	100	23.34	100			3.2	100	0.18
Cinder	85.23	65.2	100	27.4	100			3.87	100	0.2
Metall fraction	8.7	1.4	0.2	-	-	95.74	43.16	0.17	0.4	-
The magnetic fraction	51.3	55.2	50.6	25.05	46.95			6.76	89.6	0.15
Non-magnetic fraction	40.0	80.2	49.2	6.77	9.89			0.96	10.0	0.36
Total:	100		100			100				100

3.4. Leaching Process for Non-Magnetic Fraction Cake with Soda Using Water, and the Determination of Optimal Conditions

A non-magnetic slag fraction was produced and averaged, with the following composition: 74 wt.% TiO_2, 1.1 wt.% Fe_2O_3, 1.01 wt.% Cr_2O_3, and 1.9 wt.% MnO_2. The titanium-containing slag had a high chromium content. The slag was sintered with soda and then leached with water to remove the chromium. The chromium spinel, when sintered with soda in an oxidizing atmosphere at above 855 °C (the melting point of calcined soda), formed sodium chromate according to the following reaction:

$$4FeCr_2O_4 + 8Na_2CO_3 + 7O_2 \rightarrow 8Na_2CrO_4 + 2Fe_2O_3 + 8CO_2\uparrow. \quad (9)$$

When it was sintered with soda, titanates, silicates, ferrates, and sodium aluminates were also formed according to the following reactions:

$$2TiO_2 + Na_2CO_3 = Na_2Ti_2O_5 + CO_2\uparrow, \quad (10)$$

$$SiO_2 + Na_2CO_3 = Na_2SiO_3 + CO_2\uparrow, \quad (11)$$

$$Al_2O_3 + Na_2CO_3 = Na_2Al_2O_4 + CO_2\uparrow, \quad (12)$$

$$Fe_2O_3 + Na_2CO_3 = Na_2Fe_2O_4 + CO_2\uparrow. \quad (13)$$

Before sintering, the non-magnetic fraction with soda was mechanically activated for a duration of 120 min. Mechanical activation was performed using an IV6 vibration abrader, up to a class of 40 microns. The main task for the activation of the non-magnetic fraction during the reduction smelting was to increase the surface and amorphization of the crystals of chromium-containing particles. This provided effective access for the leaching agent and increased the degree of chromium extraction into the solution [32–34].

After mechanical activation, a 0.04 mm class of non-magnetic fraction was sintered with soda at ratios of 1:0.5, 1:1, 1:1.5, and 1:2. The non-magnetic fractions were sintered in a Kejia chamber furnace at 950 °C at a heating rate of 10 °C/min and then held for 30 min. The sinter yield was 95.3–99.04% during the sintering of the non-magnetic fraction with a 1:0.5 soda ratio. During the sintering of the non-magnetic fraction with a 1:1 soda ratio, the sinter yield was 93.7–95.2%. During the sintering of the non-magnetic fraction with a 1:1.5 soda ratio, the sinter yield was 92.7–93.9%. During the sintering of the non-magnetic fraction with a 1:2 soda ratio, the sinter yield was 84.4–89.7%. The cake yield decreased with an increase in the soda in the ilmenite: part of the soda decomposed into Na_2O and CO_2, due to the presence of sodium bicarbonate in the soda.

After the non-magnetic fraction was sintered with soda, the cake was leached with water. We used cakes with ratios of ilmenite to soda of 1:0.5, 1:1, 1:1.5, and 1:2. The first series of experiments on leaching cakes of various ratios was performed as follows, using water. A sample of 30 g was poured into a glass beaker with water at S/L = 1:5; the temperature was 25 °C, and the leaching process was carried out for 30 min. Then, it was filtered, and the cake was washed on the filter at S/L = 1:5, dried at 100 °C, and weighed.

The volumes of the filtrate and wash water were measured, and the solutions and cakes were submitted for analysis.

In the titanium slag with soda, 94.4% of the titanium was present in the form of sodium titanates of various compositions. In the aqueous leaching process of the sinter, the crystalline structure of sodium titanates was preserved, but the substitution of Na^+ for H^+ was not observed. The ferrites and sodium manganate formed during sintering were hydrolyzed when dissolved in water and passed into the cake in the form of hematite and manganese dioxide. The changes in the extraction of chromium and sodium into the solution from the ratio of slag and soda in the initial charge are shown in Figure 19. The constant parameters of the leaching of the sinter using water when the slag ratio changed were as follows: the deposits had a solution temperature of 25 °C, an S/L ratio of 1:5, and a leaching time of 30 min.

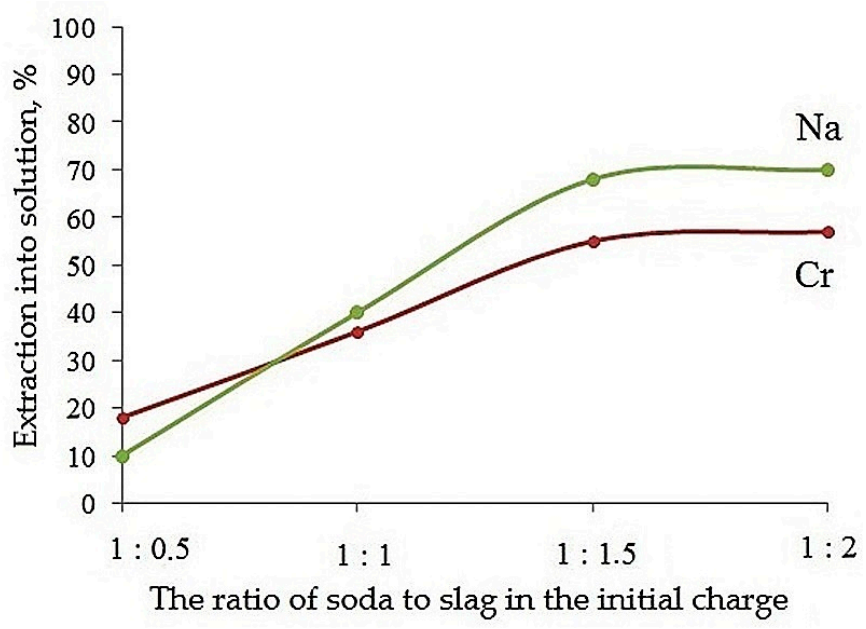

Figure 19. The dependence of the extraction of chromium and sodium into a solution during the leaching of sinters on the ratio of slag to soda in the initial charge at 25 °C.

According to the results of the first batch of experiments, the extraction of chromium and sodium into the solution gradually increased, due to the good solubility of sodium and chromium; at a ratio of 1:1.5 in the sinter, the extraction of chromium into the cake was the highest, amounting to 57%, and the extraction of sodium into the solution was 70%. At a ratio of 1:2 in the sinter, the extraction of chromium in the cake became balanced, amounting to 57%, and the extraction of sodium was 70%.

The second batch of experiments on the leaching of sinters with water at the set slag–soda ratios (1:0.5; 1:1; 1:1.5; 1:2) was carried out at a temperature of 50 °C for 30 min, with an S/L ratio of sinter to water of 1:8. After filtration, the cake was washed on a filter at S/L = 1:5, then dried at a temperature of 100 °C, and weighed. The volumes of the filtrate and rinsing water were measured, and the solutions and caps were taken for analysis. The changes in the extraction of chromium and sodium into the solution from the ratio of slag and soda in the initial charge are shown in Figure 20.

According to the results of the second batch of experiments, at a ratio of 1:1.5 in the sinter, the extraction of chromium into the solution was the highest, amounting to 58.6%. At a ratio of 1:2, the extraction of chromium into the solution became balanced, amounting to 58.5%. The extraction of sodium into the solution increased, and at a ratio of 1:2, the maximum value was 86%. Therefore, a ratio of 1:1.5 was chosen.

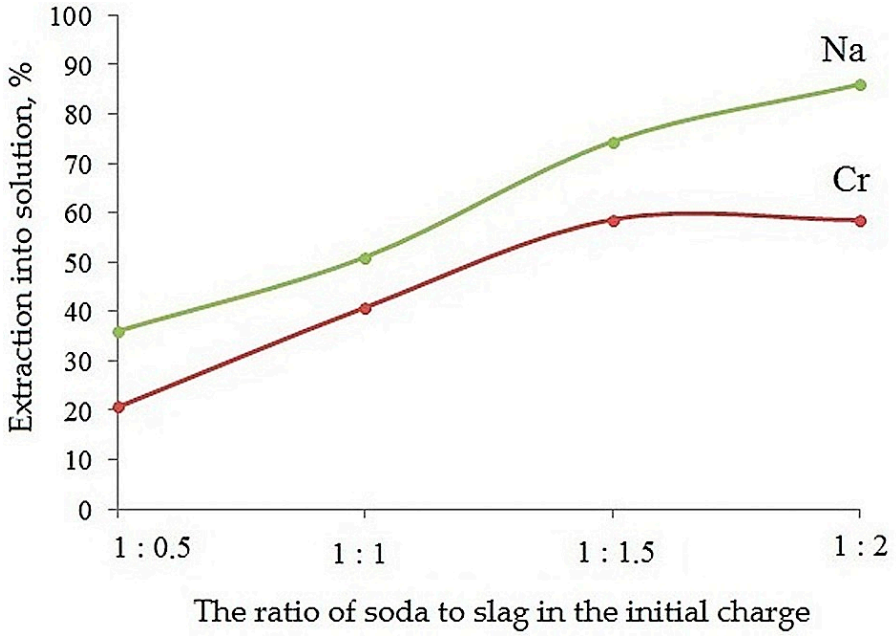

Figure 20. The dependence of the extraction of chromium and sodium into a solution during the leaching of sinters on the ratio of slag to soda in the initial charge at 50 °C.

To select the optimal leaching temperature of the sinters, experiments were conducted at temperatures of 50, 75, and 100 °C under constant experimental conditions: the ratio of slag to soda ash was 1:1.5, the time was 30 min, and the S/L ratio was 1:5. The results of the experiments are shown in Figure 21.

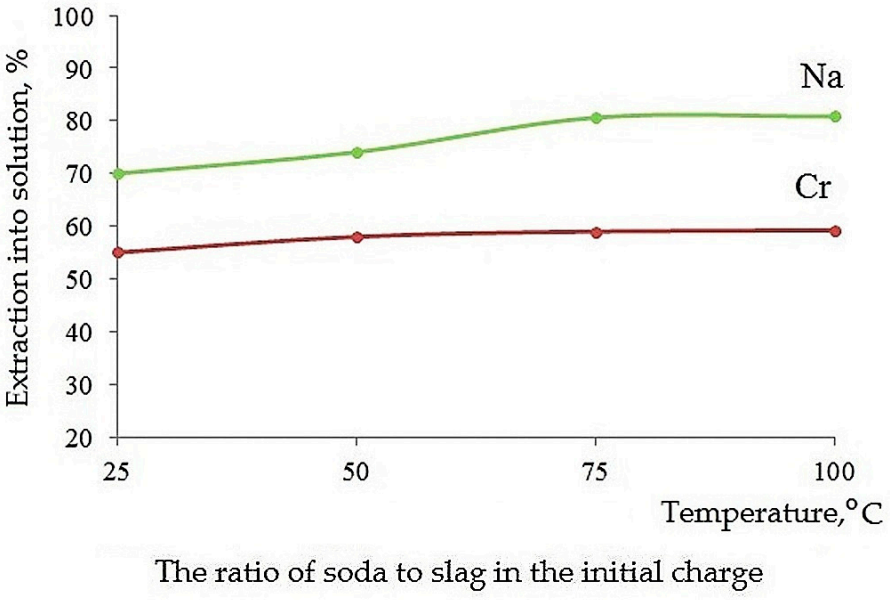

Figure 21. Dependence of chromium and sodium extraction into a solution on changes in leaching temperature.

Figure 21 shows that with increasing temperature, the extraction of sodium into the solution increased. The extraction of chromium into the solution at a temperature of 25 °C was 56.9%; at a temperature of 50 °C, it was 58.6%; at 75 °C, it was 58.8%; and at 100 °C, it was 58.9%. Therefore, the optimal temperature chosen was 50–75 °C.

Experiments were conducted to select the optimal leaching time under constant leaching conditions: a ratio of slag to soda of 1:1.5, a temperature of 50 °C, an S/L ratio of 1:5 were chosen, and the results are shown in Figure 22.

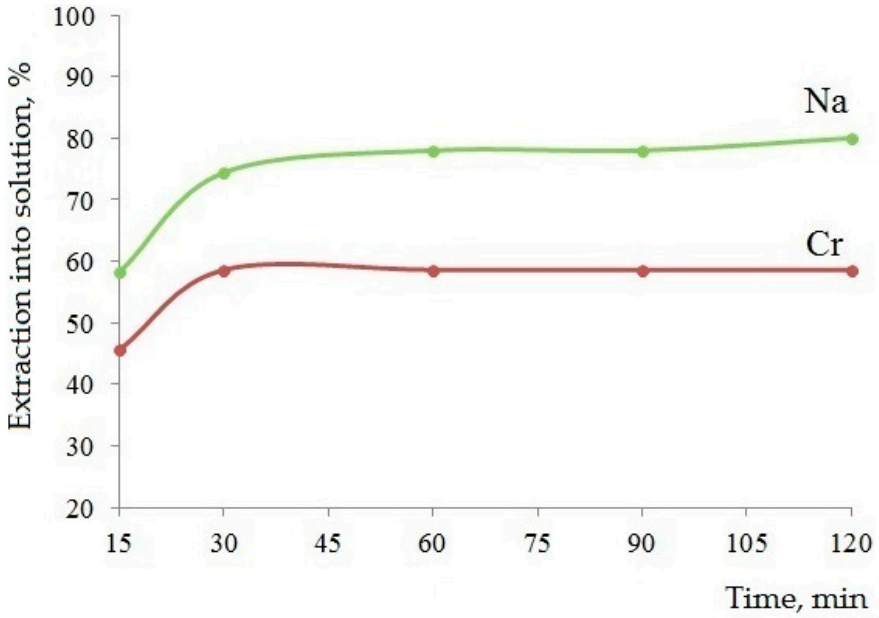

Figure 22. Extraction of chromium and sodium into a solution, depending on the duration of leaching.

Figure 22 shows that extraction into the sodium solution gradually increased from 58.2 to 80%. The extraction of chromium at 30 min was 58.6% and remained at practically the same level, and the optimal leaching time was 30 min.

Experiments to determine the S/L ratio were carried out at 1:2, 1:5, 1:8, and 1:10 under constant conditions: a temperature of 50 °C, a duration of 30 min, and a ratio of slag to soda of 1:1.5. The results of the experiments are shown in Figure 23.

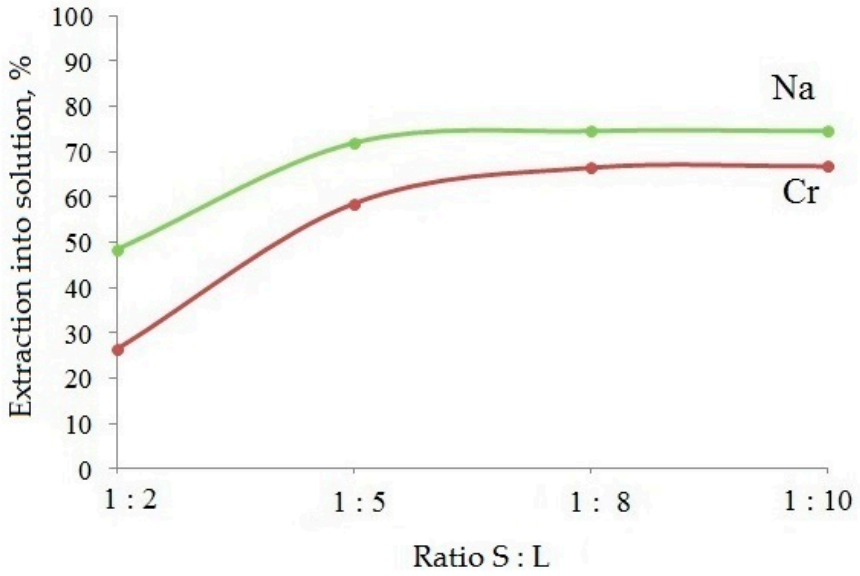

Figure 23. Extraction of chromium and sodium into a solution at 50 °C; time—30 min.

With an increase in the S/L ratio, the extraction of sodium into the solution increased from 48.5 to 74.6%, and the chromium increased and became balanced at S/L = 1:8, at 67%.

The third series of experiments to leach the cakes with water at slag-to-soda ratios of 1:0.5, 1:1, 1:1.5, and 1:2 was performed under the conditions of a ratio of cake to water of S/L = 1:8 and a temperature of 80 °C for 60 min. After filtration, the cake was washed on a filter at S:L = 1:5, then dried at 100 °C and weighed. The volumes of the filtrate and the rinsing water were measured, and the solutions and cakes were submitted for analysis.

The optimal parameters for leaching with water were a leaching temperature of 80 °C, a duration of 30 min, and a ratio of S/L = 1:8 for the cake, with a ratio of ilmenite to soda of 1:1.5. Under these conditions, the content of chromium oxide in the cake was 0.44%, corresponding to the rutile concentrate standard. The cake composition, by weight percentage, was as follows: 75.5 TiO_2, 4.0 Fe_2O_3, 1.9 MnO_2, 0.44 Cr_2O_3, 0.6 Al_2O_3, 0.86 SiO_2, 0.07 P_2O_5, and 0.025 SO_3. To reduce the chromium oxide, the cake was treated with 15% hydrochloric acid solution at T:L = 1:5, at a temperature of 90 °C for 60 min. The extraction of chromium in the solution was 84.7% and iron was 90%. In terms of oxides from acid leaching was as follows (in wt.%): 76.9 TiO_2, 0.096 Cr_2O_3, 0.13 4.0 Fe_2O_3, 0.5 MnO_2. It corresponds to the standard of titanium slag on chromium oxide.

A processing scheme was made, based on the research performed in this study to process ilmenite concentrate from the Obukhovskoye deposit in the Republic of Kazakhstan, which is presented in Figure 24.

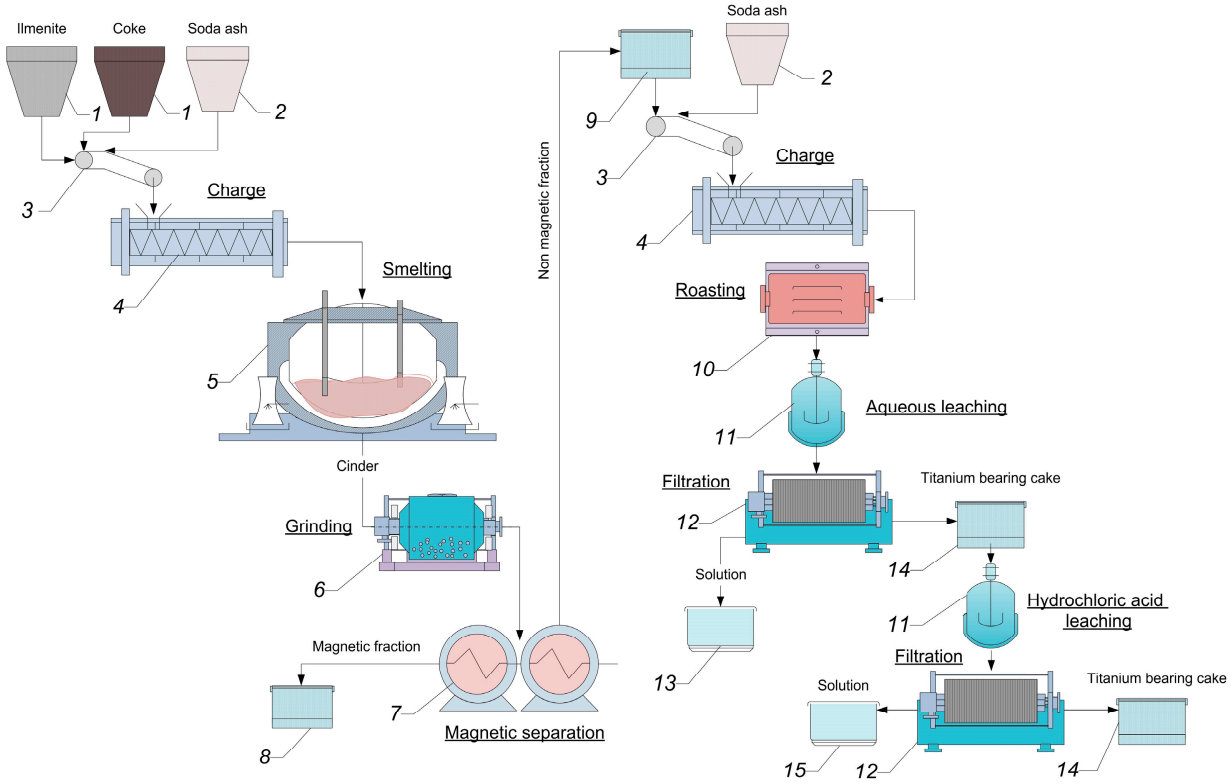

Figure 24. Scheme of processing ilmenite concentrate from the Obukhovskoye deposit.

1—bunkers for the constituent components of the charge, 2—a soda ash hopper, 3—conveyors to the loading device of the mixing drying furnaces 4, 5—an ore-thermal furnace, 6 –a mill for grinding cinder, 7—a magnetic separator, 8—a hopper for storing reduced iron and the magnetic fraction, 9—a hopper for the slag non-magnetic fraction, 10—a drum rotary kiln for roasting slag with soda ash, 11—a tank with a mixing device for water or hydrochloric acid leaching of the sinter, 12—a bag filter press, 13—a tank for sodium chromate solution, 14—a hopper for storing the titanium-containing cake, 15—a brine solution tank.

4. Conclusions

Ilmenite concentrates from the Obukhovskoye deposit are currently not being processed at titanium–magnesium plants, due to their high chromium content; however, their processing is relevant for the expansion of titanium raw materials. It is proposed in this paper that reduction smelting of the ilmenite should first be performed, with the separation of the iron and the main part of the chromium into the magnetic fraction in the form of cast iron and the obtaining of titanium with rare-earth metals into the non-magnetic slag fraction. Due to the increased content of chromium in the slag fraction, it is necessary to sinter the non-magnetic fraction with soda, followed by leaching with water to transfer the chromium and impurity components into the solution and the titanium into the cake. It can be seen that during smelting, the amount of REE separated into the non-magnetic fraction was more than 68–70%, making it possible to obtain a concentrate of REE from the non-magnetic fraction. Relevant research will be carried out in the future.

A single-stage smelting mode for the ilmenite concentrate was established: the temperature was raised to 1700 °C with a heating step of 10 °C/min with an argon supply and held for 30 min, followed by cooling to 700 °C in an argon environment.

The optimal parameters for sintering with soda were determined to be a ratio of the non-magnetic fraction to soda of 1:1.5, a temperature of 950 °C, and a holding time of 30 min. It was necessary to first subject the non-magnetic fraction to mechanical activation for 120 min. The optimal parameters for leaching with water were found to be a leaching temperature of 80 °C, a duration of 30 min, and an S/L ratio of 1:8. The aqueous leaching cake was treated with 15% hydrochloric acid solution at S/L ratio of 1:5 and at a temperature of 90 °C for 60 min. Under these conditions, the content of chromium oxide in the cake was 0.096%, corresponding to the standard for titanium slag regarding chromium oxide.

Author Contributions: Conceptualization, B.K. and A.U.; methodology, A.U., A.T. and N.S.; software, N.S.; validation, A.T. and N.S.; formal analysis, A.T.; investigation, A.T. and N.S.; resources, N.S.; data curation, A.T. and N.S.; writing—original draft preparation, A.U. and A.T.; writing—review and editing, B.K. and A.U.; visualization, A.U.; supervision, B.K.; project administration, B.K.; funding acquisition, B.K. All authors have read and agreed to the published version of the manuscript.

Funding: This research was funded by the Science Committee of the Ministry of Science and Higher Education of the Republic of Kazakhstan, Program-Targeted Funding BR21882140.

Data Availability Statement: The original contributions presented in the study are included in the article, further inquiries can be directed to the corresponding author.

Acknowledgments: We would like to thank the Ministry of Science and Higher Education of the Republic of Kazakhstan.

Conflicts of Interest: The authors declare no conflicts of interest.

References

1. Sun, H.; Wang, J.; Dong, X.; Xue, Q. A literature review of titanium metallurgical processes. *Hydrometallurgy* **2011**, *108*, 177–188. [CrossRef]
2. Akhmetova, K.S.; Kenzhaliev, B.K.; Trebukhov, S.A.; Nitsenko, A.V.; Burabaeva, N.M. Achievements in the titanium production development. *Metalurgija* **2020**, *59*, 567–570.
3. Alipovna, M.A.; Karaulovich, K.A.; Vladimirovich, P.A.; Zhanuzakovich, A.Z.; Bolatovna, K.B.; Wieleba, W.; Leśniewski, T.; Bakhytuly, N. The study of the tribological properties under high contact pressure conditions of TiN, TiC and TiCN coatings deposited by the magnetron sputtering method on the AISI 304 stainless steel substrate. *Mater. Sci.-Poland* **2023**, *41*, 1–14. [CrossRef]
4. Toishybek, A.M.; Baigenzhenov, O.S.; Turan, M.D.; Kurbanova, B.; Merkibayev, Y.S. A review of extraction technologies of rare and rare earth metals from wastes generated in titanium and magnesium production. *Kompleks. Ispolzovanie Miner. Syra = Complex Use Miner. Resour.* **2023**, *327*, 64–73. [CrossRef]
5. Sapargaliev, E.M.; Azelkhanov, A.Z.; Kravchenko, M.M.; Suiekpayev, Y.S.; Dyachkov, B.A. Prospects for the Practical Value of the Integrated Development of Poor Titanium-Zirconium Placers and Weathering Crusts in Kazakhstan. *Perm J. Pet. Min. Eng.* **2021**, *21*, 17–22. [CrossRef]

6. Ultarakova, A.; Kenzhaliyev, B.; Onayev, M.; Yessengaziyev, A.; Kasymzhanov, K. Investigations of waste sludge of titanium production and its leaching by nitric acid. In Proceedings of the 19th International Multidisciplinary Scientific GeoConference SGEM 2019, Albena, Bulgaria, 28 June–7 July 2019; pp. 861–868.
7. Pownceby, M.I.; Fisher-White, M.J. Chemical variability in chrome spinel grains from magnetically fractionated ilmenite concentrates: Implications for processing. *Miner. Process. Extr. Met.* **2006**, *115*, 213–223. [CrossRef]
8. Lv, J.-F.; Zhang, H.-P.; Tong, X.; Fan, C.-L.; Yang, W.-T.; Zheng, Y.-X. Innovative methodology for recovering titanium and chromium from a raw ilmenite concentrate by magnetic separation after modifying magnetic properties. *J. Hazard. Mater.* **2017**, *325*, 251–260. [CrossRef] [PubMed]
9. Ahmad, S.; Rhamdhani, M.A.; Pownceby, M.I.; Bruckard, W.J. Selective sulfidising roasting for the removal of chrome spinel impurities from weathered ilmenite ore. *Int. J. Miner. Process.* **2016**, *146*, 29–37. [CrossRef]
10. Steenkamp, J.D.; Pistorius, P.P. Kinetics of chromite vs. ilmenite magnetization during oxidative roasting of ilmenite concentrates. *J. South. Afr. Inst. Min. Metall.* **2003**, *103*, 501–507.
11. Nell, J.; Hoed Den, P. Separation of chromium oxides from ilmenite by roasting and increasing the magnetic susceptibility of Fe2O3-FeTiO3 (ilmenite) solid solutions. In *Proceedings of Heavy Minerals 1997*; Robinson, R.E., Ed.; South African Institute of Mining and Metallurgy: Johannesburg, South Africa, 1997; pp. 75–78.
12. Naimanbayev, M.A.; Ulasyuk, S.M.; Smirnov, K.M.; Onayev, M.I.; Kasymzhanov, K.K. Composition and technological properties of ilmenite concentrate with a high chromium content. *Kompleks. Ispolz. Miner. Syra Complex Use Miner. Resour.* **2016**, *2*, 33–39.
13. Tuleutay, F.; Trebukhov, S.; Nitsenko, A.; Burabayeva, N.; Akhmetova, K. A difficulty to process a low quality titano-ferrite concentrates. *Kompleks. Ispolzovanie Miner. Syra = Complex Use Miner. Resour.* **2018**, *307*, 77–86. [CrossRef]
14. Allen, N.R. Effect of roasting temperature on the magnetism of ilmenite. *Phys. Sep. Sci. Eng.* **2003**, *12*, 103–121. [CrossRef]
15. Krysenko, G.; Epov, D.; Medkov, M.; Merkulov, E. Studying of possibility for breakdown of ilmenite concentrate with ammonium sulphate. *Kompleks. Ispolzovanie Miner. Syra = Complex Use Miner. Resour.* **2020**, *312*, 22–30. [CrossRef]
16. Steenkamp, J.D.; Pistorius, P.C.; Allen, N.R. Reflections on ilmenite roasting and magnetic separation. *Heavy Miner. Soc. Min. Metall. Explor.* **2005**, *2005*, 133–141.
17. Song, B.; Huang, P.; Ma, Y.; Song, Z.; He, Z. Pelletization performance of Panzhihua ilmenite concentrate. *MATEC Web Conf.* **2019**, *277*, 03003. [CrossRef]
18. Lv, W.; Lv, X.; Xiang, J.; Zhang, Y.; Li, S.; Bai, C.; Song, B.; Han, K. A novel process to prepare high-titanium slag by carbothermic reduction of pre-oxidized ilmenite concentrate with the addition of Na_2SO_4. *Int. J. Miner. Process.* **2017**, *167*, 68–78. [CrossRef]
19. Lv, W.; Lv, X.; Xiang, J.; Wang, J.; Lv, X.; Bai, C.; Song, B. Effect of pre-oxidation on the carbothermic reduction of ilmenite concentrate powder. *Int. J. Miner. Process.* **2017**, *169*, 176–184. [CrossRef]
20. Xu, M.; Guo, M.; Zhang, J.; Wan, T.; Kong, L.J. Beneficiation of titanium oxides from ilmenite by self-reduction of coal bearing pellets. *Iron. Steel Res. Int.* **2006**, *13*, 6–9. [CrossRef]
21. El-Tawil, S.Z.; Morsi, I.M.; Yehia, A.; Francis, A.A. Alkali reductive roasting of ilmenite ore. *Can. Metall. Q.* **1996**, *35*, 31–37. [CrossRef]
22. Zulfiadi, Z.; Rifda, D.; Toto, Y.; Imam, S.; Taufiq, H. Carbothermic Reduction of Ilmenite Concentrate with Sodium Carbonate Additive to Produce Iron Granules and High Titania Containing Slag. *Metals* **2022**, *12*, 963. [CrossRef]
23. Bisaka, K.; Goso, X.; Thobadi, I. Improved Ilmenite Smelting Process. WO2017087997A1, 26 May 2017. Available online: https://patents.google.com/patent/WO2017087997A1/en (accessed on 5 February 2024).
24. Fisher-White, M.J.; Freeman, D.E.; Grey, I.E.; Lanyon, M.R.; Pownceby, M.I.; Sparrow, G.J. Removal of chrome spinels from Murray Basin ilmenites by low temperature roasting. *Miner. Process. Extr. Met.* **2007**, *116*, 123–132. [CrossRef]
25. Ahmad, S.; Rhamdhani, M.A.; Pownceby, M.I.; Bruckard, W.J. Thermodynamic assessment and experimental study of sulphidation of ilmenite and chromite. *Trans. Inst. Min. Metall.* **2014**, *123*, 165–177. [CrossRef]
26. Bruckard, W.J.; Pownceby, M.I.; Smith, L.K.; Sparrow, G.J. Review of processing conditions for Murray Basin ilmenite concentrates. *Miner. Process. Extr. Met.* **2015**, *124*, 47–63. [CrossRef]
27. Winter, J.D. ERMS roasting process: Technology for the separation of high grade ilmenite from Murray Basin heavy mineral concentrate. In Proceedings of the Extended Abstracts of the Murray Basin Mineral Sands Conference, Mildera, Australia, 21–23 April 1999; Geoscientists Bulletin No 26. Steward, R., Ed.; The Australia Institute of Geoscience: Mildera, Australia; pp. 125–128.
28. Ahmad, S.; Rhamdhani, M.A.; Pownceby, M.I.; Bruckard, W.J. Exploratory Study of Separation of Sulphidised Chrome Spinels from Reduced Ilmenite. *Minerals* **2022**, *12*, 1252. [CrossRef]
29. Huang, R.; Lv, X.W.; Bai, C.G.; Deng, Q.Y.; Ma, S.W. Solid state and smelting reduction of Panzhihua ilmenite concentrate with coke. *Can. Met. Q.* **2012**, *51*, 434–439. [CrossRef]
30. Krogerus, H.; Makela, P.; Saarenmaa, J.; Pisila, S.; Palovaara, P. Method for Producing Titanium Oxide-Containing Slag and Pig Iron from Ilmenite and a Plant. WO2016120529A1, 4 August 2016. Available online: https://patents.google.com/patent/WO2016120529A1/en (accessed on 5 February 2024).
31. Francis, A.A.; El-Midany, A.A. An assessment of the carbothermic reduction of ilmenite ore by statistical design. *J. Mater. Process. Technol.* **2008**, *199*, 279–286. [CrossRef]
32. Dewan, M.A.R.; Zhang, G.; Ostrovski, O. Carbothermal reduction of a primary ilmenite concentrate in different gas atmospheres. *Metall. Trans. B* **2010**, *41B*, 182–192. [CrossRef]

33. Gladyshev, S.V.; Abdulvaliev, R.A.; Kenzhaliev, B.K.; Dyusenova, S.B.; Imangalieva, L.M. Development of a technology for producing chromite concentrate from sludge tailings. *Complex Use Miner. Resour.* **2018**, *1*, 12–17.
34. Chen, G.; Jiang, Q.; Li, K.; He, A.; Peng, J.; Omran, M.; Chen, J. Simultaneous removal of Cr(III) and V(V) and enhanced synthesis of high-grade rutile TiO_2 based on sodium carbonate decomposition. *J. Hazard. Mater.* **2020**, *388*, 122039. [CrossRef]